Journal of Medicinal Chemistry

Article

Cite This: J. Med. Chem. XXXX, XXX, XXX−XXX

pubs.acs.org/jmc

N-Benzyl/Aryl Substituted Tryptanthrin as Dual Inhibitors of Indoleamine 2,3-Dioxygenase and Tryptophan 2,3-Dioxygenase

Dan Yang,[†] Shengnan Zhang,[†] Xin Fang,[†] Leilei Guo,[†] Nan Hu,[†] Zhanling Guo,[†] Xishuai Li,[†] Shuangshuang Yang,[†] Jin Chao He,[†] Chunxiang Kuang,*[,‡] and Qing Yang*[,†]

[†]State Key Laboratory of Genetic Engineering, Department of Biochemistry, School of Life Sciences, Fudan University, Songhu Road 2005, Shanghai 200438, China

[‡]Department of Chemistry, Tongji University, Siping Road 1239, Shanghai 200092, China

Supporting Information

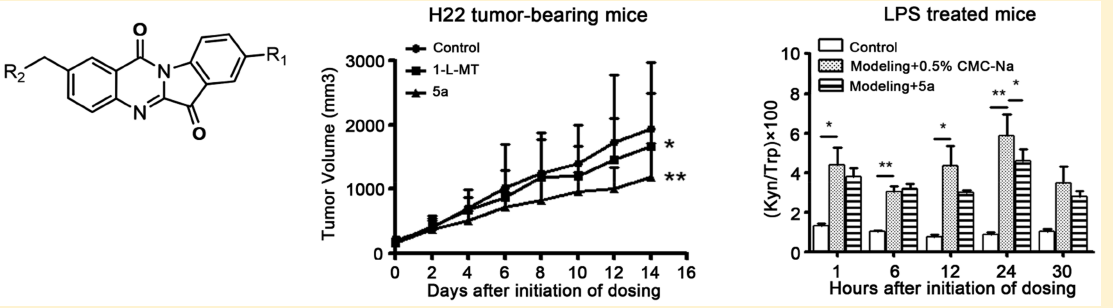

ABSTRACT: Indoleamine 2,3-dioxygenase 1 (IDO1), which catalyzes the initial and rate-limiting step of the kynurenine pathway of tryptophan catabolism, has emerged as a key target in cancer immunotherapy because of its role in enabling cancers to evade the immune system. Tryptophan 2,3-dioxygenase (TDO) and indoleamine 2,3-dioxygenase 2 (IDO2) catalyze the same reaction and play a potential role in cancer immunotherapy. Starting from our previously discovered tryptanthrin IDO1 inhibitor scaffold, we synthesized novel *N*-benzyl/aryl substituted tryptanthrin derivatives and evaluated their inhibitory efficacy on IDO1, TDO, and IDO2. Most compounds showed similar high inhibitory activities on both IDO1 and TDO, which were significantly superior over that of IDO2 with magnitude difference. We showed that *N*-benzyl/aryl substituted tryptanthrin directly interacted with IDO1, TDO, and IDO2, significantly augmented the proliferation of T cells in vitro, blocked the kynurenine pathway, and suppressed tumor growth when administered to LLC and H22 tumor-bearing mice.

INTRODUCTION

Essential amino acid tryptophan (Trp) is metabolized along the kynurenine (Kyn) and serotonin (5-HT) pathways, producing an array of Kyn metabolites such as kynurenic acid, 3-hydroxykynurenine, quinolinic acid (QUIN), and nicotinamide adenine dinucleotide, as well as a variety of neuroactive substances including well-known neurotransmitters serotonin and melatonin.[1] The 5-HT pathway of Trp metabolism is associated with psychiatric disorders including major depressive disorder and schizophrenia.[2] The kynurenine pathway (KP) of Trp metabolism not only is implicated in neurodegenerative diseases and neurological disorders but also plays a central role in tumor-induced immunosuppression.[3]

The first and rate-limiting enzymes of the KP are indoleamine 2,3-dioxygenase 1 (IDO1) (EC 1.13.11.52), tryptophan 2,3-dioxygenase (TDO) (EC 1.13.11.11), and indoleamine 2,3-dioxygenase 2 (IDO2) (EC 1.13.11). Three dioxygenases have different tissue distribution and different physiological roles.[4] The first enzyme, IDO1, is a monomeric heme-containing enzyme that is widely distributed in various tissues of mammals. IDO1 has been linked to energy homeostasis and immune defense that is relevant to both neurological diseases and cancer.[5] The second enzyme is tryptophan 2,3-dioxygenase (TDO, encoded by the TDO2 gene), which is a tetrameric heme-containing enzyme. In contrast, TDO constitutively expresses at high levels in the liver, where it regulates systemic Trp levels and plays a comparable role in cancer immunology.[6,7] TDO is also expressed in the brain and within the central nervous system (CNS), and TDO is involved in neurogenesis and can modulate anxiety-like behaviors in mice.[8] In 2007, a monomeric heme-containing enzyme homologous to IDO1 was identified and named IDO2.[9−11] IDO2 is primarily expressed in liver, kidney tubules, and reproductive tracts (e.g., epididymis, spermatozoa) apart from various cell lines such as pancreatic, gastric, colon, and kidney carcinoma.[9,10] IDO2 exhibits nonredundant roles in adaptive immunity[12] and autoimmunity,[13] but its functions within the CNS are not clear.

Overactivation of the three dioxygenases, which is mainly associated with the upregulation of the KP and the production

Received: July 4, 2019

DOI: 10.1021/acs.jmedchem.9b01079
J. Med. Chem. XXXX, XXX, XXX−XXX

of excitotoxin QUIN, has been proved being implicated in the pathogenesis of cancer immunoescape, neuroinflammatory disorders, neurodegenerative disorders (Alzheimer's disease), and depression.[14] The immunosuppressive effect of IDO1 is attributed to the depletion of Trp and the increase in Kyn, which involves three effector pathways of GCN2, mTOR, and aryl hydrocarbon receptor (AhR),[15] while the immunosuppressive effect imparted by TDO and IDO2 mainly is attributed to AhR.[16−18]

Since IDO1 plays a major role in this context, it has emerged as a promising therapeutic target, prompting a search for highly active inhibitors. Various chemical inhibitors of IDO1 have been developed and tested for their immunostimulatory effects in preclinical settings, including methylthiohydantoin-tryptophan, brassinin, annulin B, exiguamine A and their corresponding derivatives, INCB023843, 4-phenyl-1,2,3-triazole, and tryptanthrin.[19−29] 1-Methyl-D-tryptophan (also known as indoximod or NLG8189), epacadostat (also known INCB24360), NLG919 (also known as GDC-0919), and F001287 have entered clinical development.[30−32] However, the failure of clinical trials of several IDO1 inhibitors including INCB24360, NLG919, and F001287 has been known since the winter of 2017. Thus, discovery of new IDO1 inhibition strategy has become extremely urgent. TDO inhibitors are also being developed, the TDO-specific inhibitor LM10 has been shown to mediate therapeutically relevant immunostimulatory effects in mice with TDO-expressing tumors,[33] although for the moment only in preclinical settings. However, only a few compounds are known to be IDO2 inhibitors;[7,34,35] 1-L-MT is a more potent IDO2 inhibitor than D-1-MT.[36,37] By screening of a library of FDA-approved drugs in the HEK293T cells transfected by mouse IDO2 gene, the proton pump drug tenatoprazole was found to be an efficacious mIDO2 inhibitor (with an IC_{50} value of 1.8 μM) but not for IDO1 or TDO inhibition.[38]

Our previous studies have shown that natural product tryptanthrin (indolo[2,1-*b*]quinazolin-6,12-dione) is a potent IDO1 inhibitor scaffold; several tryptanthrin derivatives have IDO1, TDO, and IDO2 inhibitory activities.[29,39,40] Herein, we designed and synthesized novel *N*-benzyl/aryl substituted tryptanthrins and evaluated their IDO1, TDO, and IDO2 inhibitory potencies in both enzymatic and cellular levels. Among these *N*-benzyl/aryl substituted tryptanthrin derivatives, compound **5a** was chosen for further in vitro and in vivo studies because of its improved physical chemical properties. We examined the interactions of **5a** with IDO1, TDO, and IDO2, the effects of **5a** on the proliferation of T cells in vitro, the blockade of KP in vivo, and the tumor growth in tumor-bearing mice.

RESULTS AND DISCUSSION

Chemistry. The synthesis of *N*-benzyl/aryl substituted tryptanthrins derivatives is described in Schemes 1 and 2. 6-Methylisatoic anhydride **2** was synthesized by Baeyer−Villiger oxidation rearrangement of 5-methylisatin **1** utilizing 3-chloroperbenzoic acid (mCPBA) as an oxygen donor. Subsequently, compound **4** was achieved by an efficient two-step process of condensation and NBS bromination. Then nucleophilic substitution on benzyl bromide of **4** with various amines in the presence of a catalytic quantity of KI provided **5a−f** in 35−67% yield. Compound **8** was obtained by the similar method with **3**. It is noted that **9a−f** was afforded with

Scheme 1. Synthetic Route To Generate *N*-Benzyl Substituted Tryptanthrins Derivative 5[a]

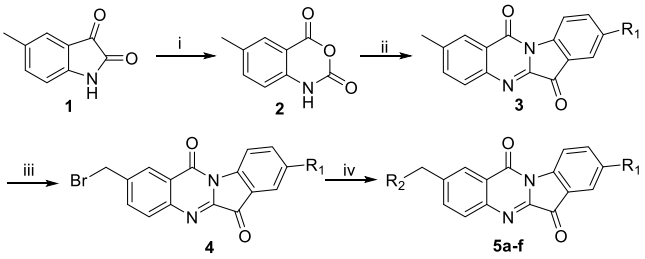

[a]Reaction conditions: (i) m-CPBA, CH_2Cl_2, rt; (ii) 5-fluoroisatin or isatin, Et_3N, toluene, reflux; (iii) NBS, AIBN, CH_2Cl_2, reflux; (iv) Et_3N, KI, DMF, amine.

$Pd(OAc)_2$ as catalyst owing to the worse reactivity of aryl bromide compared to benzyl bromide.

Optimal Bioassay Systems of IDO1, TDO, and IDO2. Table 1 and Table 2 respectively describe our enzymatic and cellular assays of IDO1, TDO, and IDO2 inhibitory activity of small molecules, which includes the cell line and the composition of the assay solution.[29,39−41]

The bioassay of IDO1 has been well documented, including several enzymatic assays by fluorescence method[42−45] and the cellular assay using interferon-γ (IFN-γ) stimulated HeLa cell line.[41] In contrast to IDO1, bioassays of TDO and IDO2 have not been sufficiently studied; the preparation of active recombinant hTDO and hIDO2, enzymatic assay conditions such as pH value, the compositions of incubation medium, and the specificity of cell line used in cellular assay have not been addressed in detail.[42−45] For example, the cellular TDO inhibition assay has been routinely performed in A172 cell line.[42−44] Yet A172 is not a specific tool for cellular assay of TDO because it expresses IDO1, IDO2, and TDO that all contribute to the conversion of L-Trp to *N*-formyl kynurenine (NFK). Recently, our group has established optimal hIDO2 and hTDO bioassay systems[39,40] as summarized in Tables 1 and 2.

IDO1, IDO2, and TDO Inhibitory Activities of *N*-Benzyl/Aryl Substituted Tryptanthrins. The known IDO1 selective inhibitors exhibit different inhibition types; for example, 4PI[46,47] and EOS200271[48] are noncompetitive IDO1 inhibitors, Amg-1[49] is competitive type, while BMS-986205[50] is irreversible type. Herein, the detailed kinetic analyses of these *N*-benzyl/aryl substituted tryptanthrins were performed based on plotting of the reciprocal of the reaction velocity ($1/V$) against the inhibitor concentration ([I]). The test compounds were categorized as reversible inhibitors. Despite having the same structural skeleton, the test compounds exhibited different types of inhibition. As shown in Table 3, most compounds had a kinetic graphical mode that suggested uncompetitive inhibition of IDO1, TDO, and IDO2. The K_i values were evaluated by plotting [S]/V against [I], where [S] represents the substrate concentration and V represents the reaction velocity (Table 3).

As shown in Table 4, most *N*-benzyl/aryl substituted tryptanthrins displayed similar IDO1 and TDO inhibitory activities superior over IDO2 inhibitory activity with magnitude difference. The IDO1 and TDO inhibitory activities of most tryptanthrins were similar in both enzymatic and cellular assays. From a structural point of view, the *N*-benzyl substituted tryptanthrins showed higher IDO1, IDO2, and

DOI: 10.1021/acs.jmedchem.9b01079
J. Med. Chem. XXXX, XXX, XXX−XXX

Scheme 2. Synthetic Route To Generate *N*-Aryl Substituted Tryptanthrins Derivative 9[a]

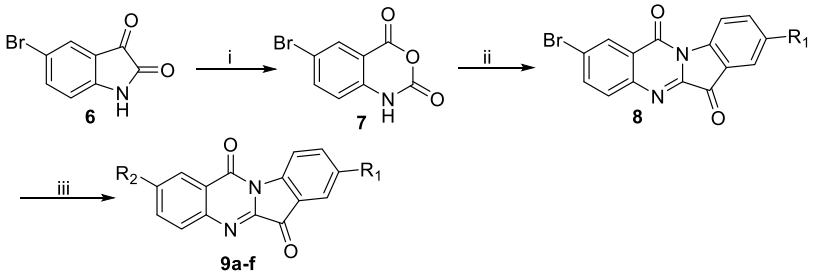

[a]Reaction conditions: (i) m-CPBA, CH_2Cl_2, rt; (ii) 5-fluoroisatin or isatin, Et_3N, toluene, reflux; (iii) $Pd(OAc)_2$, BINAP, amine, Cs_2CO_3, toluene, reflux, 16 h.

Table 1. In Vitro Enzymatic IDO1, TDO, and IDO2 Inhibition Assays

assay	class	reagent	final concentration
IDO1[a]	reducing agent	ascorbic acid	40 mM
		methylene chloride	20 μM
		catalase	200 μg/mL
	substrate	L-Trp	400 μM
	solvent	KPB[b] buffer (pH = 6.5)	50 mM
TDO[c]	reducing agent	ascorbic acid	40 mM
		methylene chloride	20 μM
		catalase	200 μg/mL
	substrate	L-Trp	400 μM
	solvent	KPB buffer (pH = 7.0)	50 mM
IDO2[d]	reducing agent	ascorbic acid	40 mM
		methylene chloride	20 μM
		catalase	200 μg/mL
	substrate	L-Trp	30 mM
	solvent	KPB buffer (pH = 7.5)	50 mM

[a]In vitro enzymatic IDO1 inhibition assay was performed as in ref 29, with some modifications. [b]KPB: potassium phosphate buffer. [c]In vitro enzymatic TDO inhibition assay was performed as in ref 40, with some modifications. [d]In vitro enzymatic IDO2 inhibition assay was performed as in ref 39, with some modifications.

Table 2. In Vitro Cellular IDO1, TDO, and IDO2 Inhibition Assays

assay	cell line	expression of IDO1, TDO, IDO2	reagent
IDO1[a]	HeLa	IDO1 expressed by IFN-γ induction	DMEM
TDO[b]	HEK293	TDO expressed by transient transfection of pcDNA3.1(+)-hTDO	DMEM supplemented with 200 μM L-Trp
IDO2[c]	U87 MG	IDO2 expressed by transient transfection of pcDNA3.1(+)-hIDO2	DMEM supplemented with 200 μM L-Trp

[a]In vitro cellular IDO1 inhibition assay was performed as in refs 29 and 41, with some modifications. [b]In vitro cellular TDO inhibition assay was performed as in ref 40, with some modifications. [c]In vitro cellular IDO2 inhibition assay was performed as in ref 39, with some modifications.

TDO inhibitory activities when compared to their *N*-aryl substituted analogues. All the tested *N*-benzyl/aryl substituted tryptanthrins displayed much higher inhibitory efficiencies in the cell-based assays than in the enzymatic assays. Usually, cellular IC_{50} values of IDO1 inhibitors are all much lower than the enzymatic IC_{50} values, for example, 1-L-MT (enzymatic IC_{50} = 380 μM, cellular IC_{50} = 18.4 μM),[51] INCB24360 (enzymatic IC_{50} = 71.8 nM, cellular IC_{50} = 7.1 nM),[41] and 4-phenyl-1,2,3-triazole 1 (enzymatic IC_{50} = 83 μM, cellular IC_{50} = 8.9 μM).[52] Similar tendency is observed in TDO inhibitors. The enzymatic IC_{50} value of TDO inhibitor LM10 is 18.7 μM,[40] which is 30-fold higher than its cellular IC_{50} value (0.62 μM).[33] Furthermore, the enzymatic IC_{50} value of TDO inhibitor 680C91 (1.3 μM)[53] is nearly 5-fold higher than its cellular IC_{50} value (0.28 μM).[33] However, IDO1 inhibitor EOS200271 displays better enzymatic IC_{50} value than its cellular IC_{50} value (enzymatic IC_{50} = 0.41 or 0.15 μM, cellular IC_{50} = 1.8 μM).[48] BMS-986205 exhibits equal enzymatic and cellular inhibitory activities (enzymatic IC_{50} = 1.1 nM, cellular IC_{50} = 0.5 nM).[54] The reason behind this remains unclear. However, the reagents, pH value, and the activities of the enzymes are different in the enzymatic assay and cellular assays. In general, a good correlation between the enzymatic assay and cellular assay is observed.

Under the same conditions, 1-L-MT showed weaker inhibitory activities than *N*-benzyl/aryl substituted tryptanthrins on IDO1 and IDO2 in both enzymatic and cellular assays but had no inhibitory activity on TDO. 1-L-MT was reported to be a substrate rather than an inhibitor for TDO.[40,55] INCB24360 showed IDO2 and TDO enzymatic inhibitory activities with IC_{50} values of 10.34 μM and 64.5 μM, which were consistent with their previous report.[56] The cellular IC_{50} of INCB24360 to TDO was tested to be 0.261 μM. Overall, our data demonstrate that *N*-benzyl/aryl substituted tryptanthrins being tested are potent IDO1/TDO dual inhibitors, while 1-L-MT and INCB24360 are IDO1 selective inhibitors. To date, most known inhibitors are IDO1 selective, IDO1/TDO dual inhibitor is rare, and RG-70099 (Roche/CuraDev) has little information disclosed in the biomedical literature.[50]

Interactions between 5a and hIDO1, hIDO2, hTDO. To clarify the potent interaction between the *N*-benzyl/aryl substituted tryptanthrins and IDO1, TDO, and IDO2, human recombinant IDO1, TDO, and IDO2 were respectively prepared and Carr–Purcell–Meiboom–Gill (CPMG) and saturation transfer difference (STD) experiments were operated. T1ρ NMR spectra for compound **5a**, in the absence (red) or in the presence of target protein (cyan), are shown in Figure 1A; the difference between the red and cyan signals indicates that the NMR signals for compound **5a** are changed due to the presence of the target protein, which means compound **5a** interacts with the target protein. The CPMG experiments show that compound **5a** directly interacts with hIDO1, hTDO, and hIDO2. Additionally, STD spectrum of compound **5a** in the presence of hIDO1, hTDO, and hIDO2 shows clear signals, indicating that **5a** directly interacts with

DOI: 10.1021/acs.jmedchem.9b01079
J. Med. Chem. XXXX, XXX, XXX−XXX

Table 3. IDO1, IDO2, and TDO Inhibitory Types and K_i Values of *N*-Benzyl/Aryl Substituted Tryptanthrins

Compound	R_1	R_2	Type of inhibition			Ki (μM)		
			IDO1	IDO2	TDO	IDO1	IDO2	TDO
5a	F		U[a]	MC[b]	U	2.64	6.32	0.31
5b	F		N[c]	U	U	4.12	1.96	0.12
5c	F	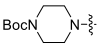	U	U	MU[d]	7.21	6.11	0.13
5d	H		U	MU	MU	5.97	8.85	0.42
5e	F		U	U	MU	0.31	4.32	0.09
5f	F		U	U	U	0.47	17.54	0.34
9a	F		N	N	MU	6.92	19.86	0.17
9b	F		U	U	MU	6.08	36.94	0.67
9c	F		U	U	U	4.34	26.79	1.56
9d	H		U	U	U	7.57	48.67	17.96
9e	F		U	N	U	8.82	45.33	1.24
9f	F		ND[e]	U	U	NI[f]	39.11	2.36
1-L-MT			C[g,h]	C[i]	ND	34[h]	425[i]	ND
INCB24360			ND	ND	U	ND	ND	21.70

[a]U: uncompetitive; [b]MC: mixed competitive. [c]N: noncompetitive. [d]MU: mixed uncompetitive. [e]ND: not detected. [f]NI: no inhibition. [g]C: competitive. [h]Inhibitory type and K_i value according to ref 57. [i]Inhibitory type and K_i value according to ref 39.

the target proteins. From a similar view, it is concluded that compound 1-L-MT weakly interacts with hIDO1 but hardly interacts with hTDO and hIDO2 (Figure 1B).

Subsequently, the heme binding study of **5a** was conducted by spectroscopic methods. Heme, a porphyrin ring with an iron at its center, is a cofactor in the active site of IDO1, which absorbs light in the UV−vis spectrum maximally at a wavelength of around 400 nm depending on the oxidation and coordination states of its iron. Inhibitors that coordinate the heme iron will shift the Soret band λ_{max}.[46] Inhibitors that do not directly coordinate the iron will only modulate the Soret band because the heme is highly sensitive to changes in the polarity of its surroundings.[46,48] As shown in Figure 2, a clear redshift of the Soret band from 405 nm (ferric IDO1) to 410 nm was observed with INCB24360 (green curve), a known as heme binding inhibitor of IDO1, while no apparent shift was observed for **5a** (blue curve). It was also noted that the absorbance of Soret band at 405 nm significantly decreased in the presence of **5a**. This result was similar to the previous report of IDO1 inhibitor EOS200271/PF-06840003,[48] indicating that **5a** does not bind to the heme iron of IDO1 and has a novel binding mode.

To date, only a few X-ray crystallography results of IDO1 inhibitor with IDO1 have been reported. The crystallization of a weak noncompetitive IDO1 inhibitor 4PI with IDO1 was first reported in 2006.[47] Later in 2014, the crystallizations of competitive IDO1 selective inhibitor Amg-1 with IDO1 were reported.[58] In 2015, a NLG919 analogue was shown to coordinate with the heme iron and to occupy both pockets A and B of IDO1.[59] It was interesting to find that this compound formed an extensive hydrogen bond network with IDO1, while noncompetitive IDO1 inhibitor EOS200271 was recently reported not to bind the heme group of IDO1.[48] Similarly, the irreversible IDO1 inhibitor BMS-986205 has been reported to bind to the apo-form of the enzyme.[60]

The present study affords CPMG and STD to be a new method besides X-ray crystallography and molecule docking to confirm the interaction of IDO1 inhibitors to IDO1.

Effect of 5a on T Cell Proliferation. The upregulation of KP can block T lymphocyte proliferation by depleting Trp locally. It has been reported that 1-L-MT and INCB24360 can

DOI: 10.1021/acs.jmedchem.9b01079
J. Med. Chem. XXXX, XXX, XXX−XXX

Table 4. IDO1, IDO2, and TDO Inhibitory Activities of *N*-Benzyl/Aryl Substituted Tryptanthrins

Compound	R_1	R_2	IC_{50} (μM)					
			Enzymatic			Cellular		
			IDO1	IDO2	TDO	IDO1	IDO2	TDO
5a	F		0.50	18.44	0.76	0.02	18.66	0.09
5b	F		0.68	31.45	0.87	0.07	3.58	0.09
5c	F		1.88	62.61	0.45	0.13	8.05	0.07
5d	H		2.52	46.86	2.41	0.18	23.29	0.18
5e	F		0.11	14.03	0.41	0.02	3.81	0.06
5f	F		0.40	39.55	0.87	0.02	16.54	0.07
9a	F		2.20	46.82	2.59	1.87	79.00	0.25
9b	F		1.19	41.63	3.15	0.76	17.76	0.29
9c	F		1.80	40.09	10.09	2.24	22.22	3.70
9d	H		8.01	82.57	6.75	2.96	48.67	0.47
9e	F		10.35	91.35	3.82	0.59	90.90	0.27
9f	F		NI[a]	79.91	6.40	NI	20.32	0.50
1-L-MT			380[b]	82.53[c]	NI	18.40[b]	56.96[c]	ND[d]
INCB24360			0.07	10.34	64.50	0.007	ND	0.26

[a]NI: no inhibition. [b]IC_{50} value according to ref 57. [c]IC_{50} value according to ref 39. [d]ND: not detected.

augment T cell function that is stimulated by tumor cells.[41,61] Here, to determine whether *N*-benzyl/aryl substituted tryptanthrins could improve T cell proliferation, we evaluated the efficacy of compound **5a** on human T cell proliferation. IFN-γ-treated IDO+ HeLa cells were cocultured with human T cells in the presence of a soluble anti-CD3 antibody and human recombinant IL-2. As shown in Figure 3, compound **5a** enhanced the proliferation of T cells stimulated with IDO+ HeLa cells, which is more effective than that of 1-L-MT. Our results clearly demonstrate that *N*-benzyl/aryl substituted tryptanthrins as highly potent IDO1/TDO dual inhibitors can reverse the suppression of T lymphocyte, but 1-L-MT has no significant effect on T cell proliferation at the same concentration.

Blockade Effect of 5a on LPS Stimulated and Basal KP in Vivo. The blockade effect of **5a** on overactivated KP was first investigated using LPS-treated mice. As shown in Figure 4, the Trp concentration in control mice at each sampling time was generally higher than that in modeling mice treated with LPS, which indicated that the control mice took more Trp than the modeling mice did because the mice were allowed ad libitum access to food and water during the experiment. In modeling mice, the KP was stimulated involving the decreased Trp level, increased Kyn level, and the enhanced Kyn/Trp ratio. The effect of **5a** on KP was analyzed at 1 h, 6 h, 12 h, 24 and 30 h after dosing. It was found that **5a** could significantly increase the Trp level at 12 h and 24 h after dosing and yet not affect the Kyn level and therefore markedly reversed the enhanced Kyn/Trp ratio at 24 h after dosing. To date, IDO1 inhibitors with different inhibition types have been developed. Structure, degree of similarity to the substrate L-Trp, and heme binding ability of inhibitors make the mode of action disparate. INCB24360 inhibits IDO1 activity in a fast and short mode, while some inhibitors show an intriguingly slow onset of inhibition.[60] Our compound exhibited inhibition at 12 and 24 h.

Further, the blockade effect of **5a** on basal KP was examined using lung tissue of naive SD rats. As shown in Figure 4E, the

DOI: 10.1021/acs.jmedchem.9b01079
J. Med. Chem. XXXX, XXX, XXX−XXX

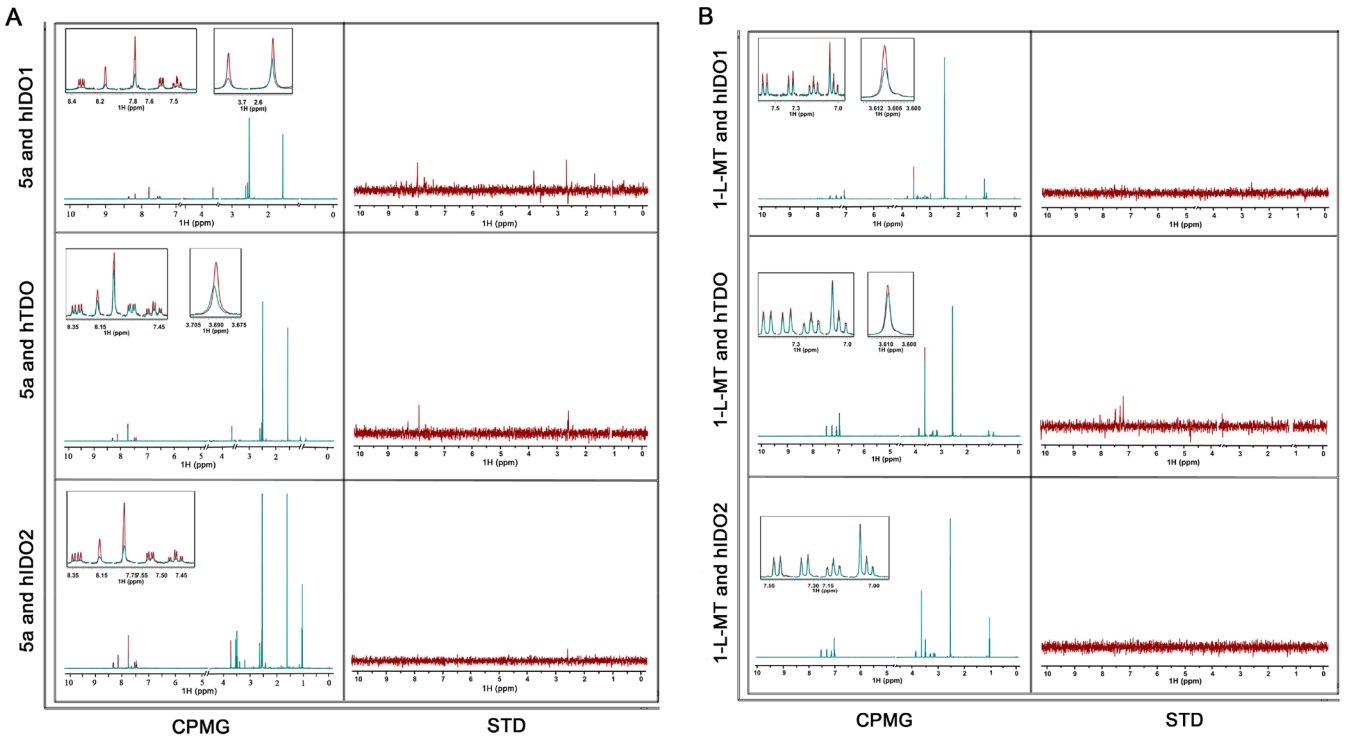

Figure 1. CPMG and STD NMR studies on interactions between **5a** and hIDO1, hTDO, and hIDO2. (A) Ligand observed T1ρ and STD spectra indicate that compound **5a** directly interacts with target proteins hIDO1, hTDO, and hTDO. (B) Ligand observed T1ρ and STD spectra indicate that compound 1-L-MT weakly interacts with target protein (hIDO1 and hTDO) but does not interact with hIDO2. Left panel: T1ρ NMR spectra for compound in the absence (red) or the presence of target protein (cyan). Right panel: STD spectrum of compound in the presence of target protein.

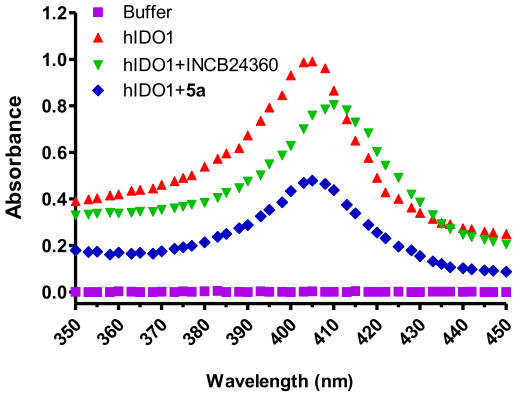

Figure 2. **5a** was evaluated for heme binding. The Soret band for ferric hIDO1 (λ_{max} = 405 nm) was recorded with or without inhibitors under normal atmospheric conditions in potassium phosphate buffer using a UV−visible spectrophotometer (path length of 1 mm).

Trp concentration in the lung tissues of **5a**-treated rats was significantly higher than that in control rats. In addition, **5a** treatment markedly reduced the Kyn level and the Kyn/Trp ratio.

Effect of 5a on Tumor Growth in LLC Tumor-Bearing Mice. LLC tumor-bearing mice were treated with compound **5a** or 1-L-MT for 2 weeks. 1-L-MT has been used as positive control in many literature studies describing the antitumor effects of IDO1 inhibitors, although it is still contentious how 1-L-MT acts in vivo; for example, 1-L-MT has been thought to act as a Trp sufficient mimetic and reverse IDO1 immune suppression in T cells.[62] However, 1-L-MT can efficiently block KP and exhibit therapeutic efficacy in vivo even if its enzymatic IC_{50} is not so good. Both **5a** and 1-L-MT retarded the growth of tumors; specifically, tumor volume was reduced 56.2% with **5a** and 33.6% with 1-L-MT (Figure 5A). **5a** significantly reduced tumor weight, while 1-L-MT showed less effect on tumor weight (Figure 5B). Although **5a** was incapable of eliciting tumor regression, it did effectively inhibit tumor growth.

Effect of 5a on Tumor Growth in H22 Tumor-Bearing Mice. H22 tumor-bearing mice were treated with **5a** or 1-L-MT for 2 weeks. Tumor volume was reduced 47.3% by **5a** and 15.8% by 1-L-MT (Figure 6A). **5a** significantly reduced tumor weight about 55.4%, while 1-L-MT showed less effect (Figure 6B). Together, the in vivo antitumor assays of **5a** in LLC or H22 tumor-bearing mice reveal the therapeutic potential of **5a** as a single agent in the treatment of tumor.

The experiments with Ido1$^{-/-}$ mice would be of benefit to clarify to what extent does the in vivo tumor growth of LLC or H22 depend on IDO1-mediated immune suppression. It has been shown that Ido1$^{-/-}$ mice have smaller tumors (about 50% reduction in tumor weight) and fewer nodules compared with wild type mice on day 9 after LLC cells injection.[63] LLC growth was attenuated in Ido1$^{-/-}$ mice, and tumors were smaller (50%, by tumor volume) than in wild type mice on day 20 after LLC tumor grafting.[64] The treatment with IDO1 siRNA significantly delayed and suppressed the LLC growth (69.78%, by tumor weight).[65] These reports indicate that mice lacking IDO1 genes were more resistant to LLC growth. However, a similar study on H22 growth has not been found. The importance of tumor-derived IDO1 in tumor immune evasion has also been confirmed by the inhibition of PAN02

DOI: 10.1021/acs.jmedchem.9b01079
J. Med. Chem. XXXX, XXX, XXX−XXX

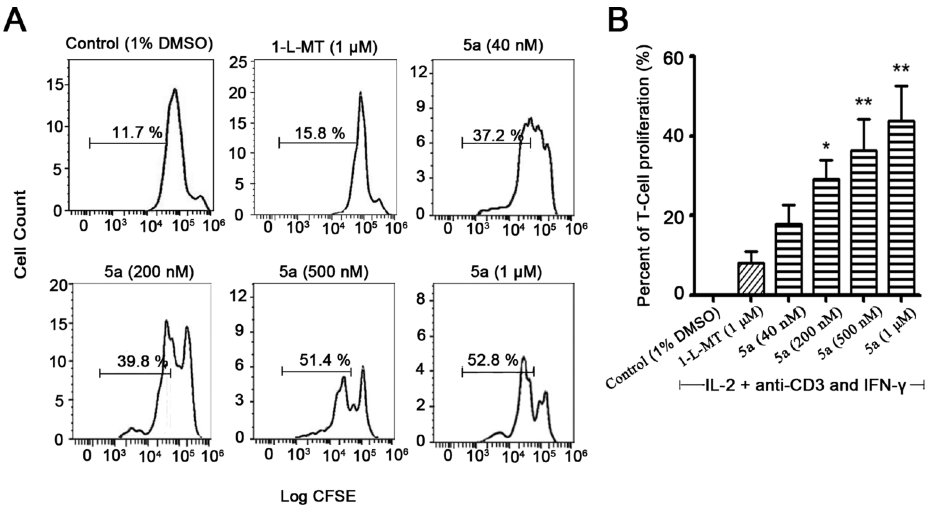

Figure 3. **5a** enhanced the proliferation of T cells stimulated by IDO1-expressing HeLa cells. (A) Effect of **5a** on T cell proliferation assayed by flow cytometry. Appropriate numbers of HeLa cells and T cells were mixed in 96-well plates and treated with 150 U/mL IL-2 and 100 ng/mL anti-CD3 antibody, as well as 60 ng/mL IFN-γ and various concentrations of **5a** as indicated for 2 days. (B) Percent of T cell proliferation. Cell proliferation was performed three times independently: (*) $P < 0.05$, (**) $P < 0.01$.

(murine pancreatic ductal adenocarcinoma cells) growth with IDO1 inhibitor INCB023843 in both wild type and Ido1$^{-/-}$ C57BL/6 mice.[21]

Blockade Effects of 5a on KP in H22 or LLC Tumor-Bearing Mice. To investigate if **5a** could efficiently block KP, the Kyn and Trp levels in the serum harvested from H22 tumor-bearing mice were examined by HPLC, and Kyn/Trp ratios were calculated. As shown in Figure 7A, the concentration of Kyn was lower in **5a** or 1-L-MT treated mice than that in control mice. In addition, mice treated with **5a** had a significant increment of Trp level, while mice treated with 1-L-MT had not (Figure 7B). As shown in Figure 7C, the Kyn/Trp ratio was significantly lower in **5a**-treated mice than in control mice.

In addition, to investigate if **5a** could efficiently block KP in tumors, the Kyn and Trp levels in the tumors harvested from LLC tumor-bearing mice were examined by LC−MS, and Kyn/Trp ratios were calculated. As shown in Figure 7D−F, no significant difference in the Trp concentrations was observed between **5a**-treated mice and control mice. Mice treated with **5a** had a significant lower Kyn concentration and Kyn/Trp ratio than control mice.

CONCLUSIONS

Although the Keytruda (PD1 antibody)/epacadostat (Incyte IDO1 inhibitor) combo crashed in the PhIII melanoma study, continued interest in IDO1 remains high. Increasing findings reinforce the need for inhibitors of IDO1, TDO, and IDO2 that may potentially be developed for therapeutic use. In this study, we have identified *N*-benzyl/aryl substituted tryptanthrins as potent IDO1 and TDO dual inhibitors. With the optimal assay method, both the enzymatic and cellular inhibitory activities of these compounds against IDO1, TDO, and IDO2 were investigated. The K_i values and inhibition types were also evaluated. Further evaluation of antitumor activity in vivo was performed with **5a**, which directly interacted with IDO1 and TDO and showed significant immunoregulation activity of promoting T cell proliferation. Testing in LLC and H22 tumor-bearing mice demonstrated that **5a** suppressed tumor growth evidently. Furthermore, blockade of basal and upregulated KP by **5a** in serum or tissues was confirmed in naive SD rats, LPS-treated mice, and tumor bearing mice. Taken together, these results led us to propose that *N*-benzyl/aryl substituted tryptanthrin is an attractive IDO1 and TDO dual inhibitor that may be used to resist the immune tolerance.

EXPERIMENTAL SECTION

General Chemistry Methods. ^{1}H NMR and ^{13}C NMR spectra were recorded in DMSO-d_6 or $CDCl_3$ with TMS as the internal standard by using a Bruker AV400 spectrometer. NMR data processing was performed with MestReNova software. ^{1}H chemical shifts are reported in δ (ppm) as s (singlet), d (doublet), dd (doublet of doublet), t (triplet), q (quartet), td (triplet of doublet), m (multiplet) and are referenced to the residual solvent signal $CDCl_3$ (7.26) or DMSO-d_6 (2.50). Coupling constants (J) are expressed in hertz (Hz). The protons of amino groups are not always indicated. High-resolution electrospray ionization mass spectra (ESI) were obtained on a VG Auto Spec 3000 or Finnigan MAT 90 instrument. Unless otherwise noted, all reagents and solvents were purchased from commercial suppliers such as Acros, Fluka, Sigma-Aldrich and used without further purification. Dry solvents were purchased as anhydrous reagents from commercial suppliers. All reactions were monitored by TLC with Huanghai GF 254 silica gel-coated plates. Column chromatography was carried out on 200−300 mesh silica gel at medium pressure.

The purity of tested compounds was determined by high performance liquid chromatography (HPLC, Shimadzu, Japan). The detection wavelength was 260 nm. HPLC analysis of the test compounds was performed using a Diamosil C18 column (150 mm × 4.2 mm i.d., 5 μm, Japan) preceded by a C18 guard column (Dikma, China). The column temperature was maintained at 30 °C at a flow rate of 1 mL/min. The mobile phase was a mixture of acetonitrile and 0.1% formic acid (10:90, v/v). The purity of tested compounds was confirmed as >95%.

General Procedure for the Synthesis of *N*-Benzyl Substituted Tryptanthrin Derivatives (5a−f). 8-Fluoro-2-methylindolo[2,1-*b*]quinazoline-6,12-dione or 2-methylindolo[2,1-*b*]-quinazoline- 6,12-dione (1 mmol), NBS (267 mg, 1.5 mmol), and AIBN (16 mg, 0.1 mmol) were added in 30 mL of carbon tetrachloride, and the mixture was stirred at 80 °C for 16 h under N_2. The solvent was removed under vacuum, and the residue was dissolved in dichloromethane (30 mL), washed with water (3 × 15 mL), dried over Na_2SO_4, and evaporated to give the compound 2-

DOI: 10.1021/acs.jmedchem.9b01079
J. Med. Chem. XXXX, XXX, XXX−XXX

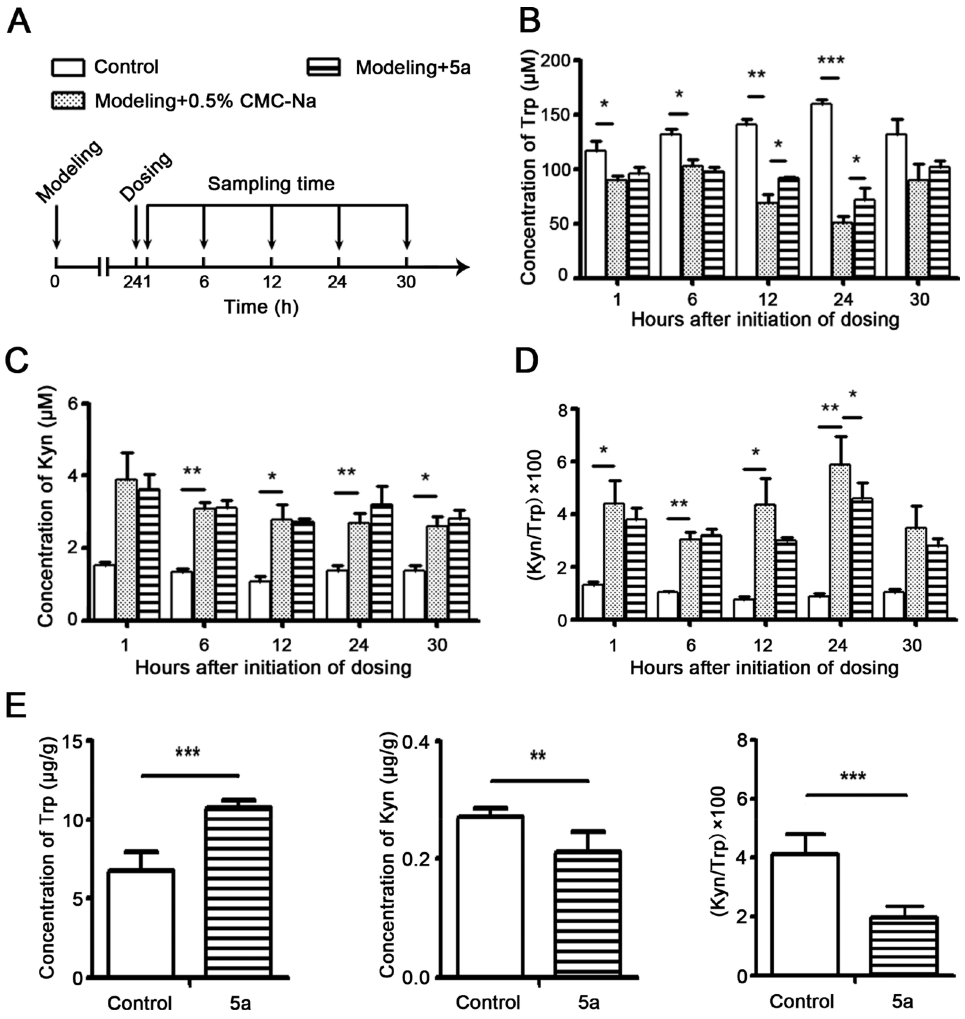

Figure 4. Blocking effects of **5a** on KP. (A–D) **5a** blocked the LPS stimulated KP in C57BL/6 mice. (A) For control and modeling, mice were challenged with saline (ip) or LPS (5 mg/kg, ip), respectively. For dosing, at 24 h after modeling, mice were treated with either 0.5% CMC-Na (0.2 mL/18 g, ig) or **5a** (60 mg/kg, ig). Sampling was 1 h, 6 h, 12 h, 24 h, 30 h after dosing, and the mice were sacrificed to harvest blood; n = 3–5 mice/group. (B–D) Kyn and Trp levels in serum were determined by HPLC, and the Kyn/Trp ratios were calculated. (E) **5a** blocked the basal KP in lung of naive SD rats. After administration of a single dose of **5a** (30 mg/kg, ig) or 0.5% CMC-Na (control, 0.2 mL per rat, ig), the naive SD rats were sacrificed to isolate lung tissues. Trp and Kyn levels were measured by LC–MS, and the Kyn/Trp ratios were calculated. (n = 3–4 rats/group): (*) $P < 0.05$, (**) $P < 0.01$, (***) $P < 0.001$.

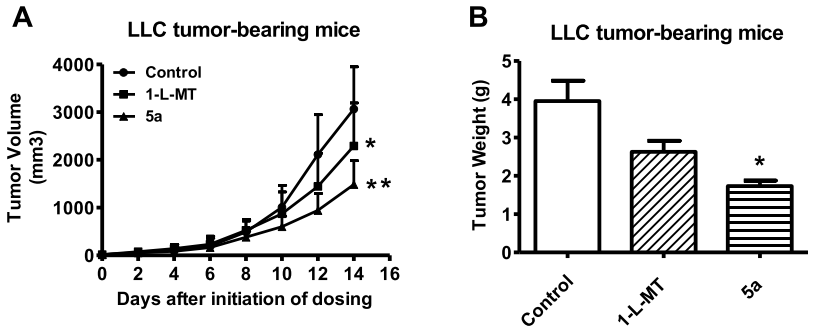

Figure 5. 5a suppressed tumor growth effectively. LLC tumor-bearing C57BL/6 mice were treated orally once daily with 0.5% CMC-Na (control), **5a** (45 mg/kg in 0.5% CMC-Na), or 1-L-MT (100 mg/kg in 0.5% CMC-Na). (A) Mean tumor volume of control (roundness), **5a**-treated mice (regular triangle), or 1-L-MT-treated mice (square) (n = 9–10 mice/group). The tumor size was measured in regular intervals. (B) Mean tumor weight of each group (n = 9–10 mice/group): (*) $P < 0.05$, (**) $P < 0.01$.

(bromomethyl)-8-fluoroindolo[2,1-*b*]quinazoline-6,12-dione or 2-(bromomethyl)indolo[2,1-*b*]quinazoline-6,12-dione as yellow solid, which could be used directly in the next step without further purification.

A suspension of 2-(bromomethyl)-8-fluoroindolo[2,1-*b*]-quinazoline-6,12-dione or 2-(bromomethyl)indolo[2,1-*b*]quinazoline-6,12-dione (1 mmol), amine (2 mmol), KI (5 mg), and triethylamine (101 mg, 1 mmol) was dissolved in DMF (5 mL) and stirred for 2 h

DOI: 10.1021/acs.jmedchem.9b01079
J. Med. Chem. XXXX, XXX, XXX–XXX

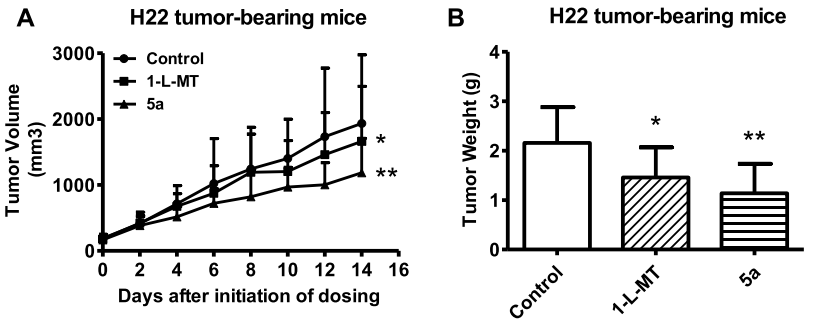

Figure 6. **5a** suppressed tumor growth effectively. H22 tumor-bearing Kunming mice were treated orally once daily with 0.5% CMC-Na (control), **5a** (45 mg/kg in 0.5% CMC-Na), or 1-L-MT (100 mg/kg in 0.5% CMC-Na). (A) Mean tumor volume of control (roundness), **5a**-treated mice (regular triangle) or 1-L-MT-treated mice (square) (n = 9−10 mice/group). The tumor size was measured in regular intervals. (B) Mean tumor weight of each group (n = 9−10 mice/group): (∗) $P < 0.05$, (∗∗) $P < 0.01$.

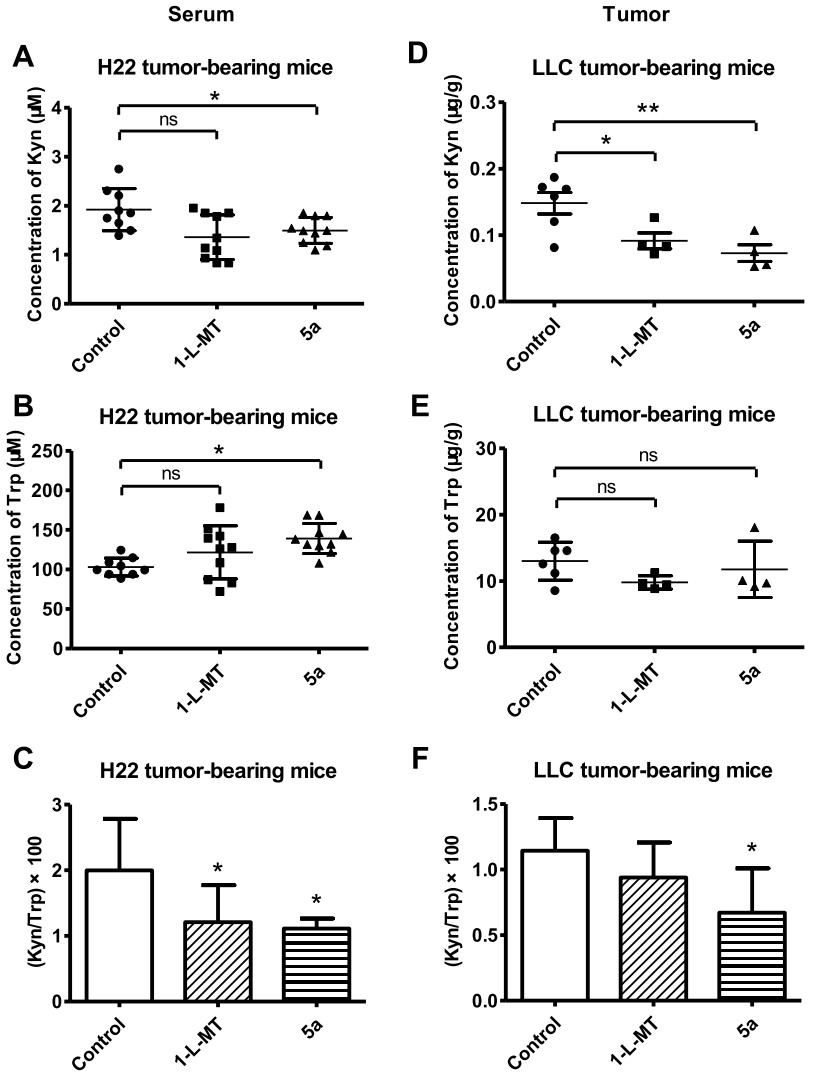

Figure 7. **5a** blocked KP in H22 and LLC tumor-bearing mice. (A−C) **5a** blocked the KP in the serum of H22 tumor-bearing mice. After administration of **5a**, the serum of H22 tumor-bearing mice was harvested. Kyn and Trp levels were determined by HPLC and the Kyn/Trp ratios were calculated. Control (roundness), **5a**-treated mice (regular triangle), or 1-L-MT-treated mice (square) (n = 9−10 mice/group). (D−F) **5a** blocked the KP in the tumor of LLC tumor-bearing mice. After administration of **5a**, the tumors of LLC tumor-bearing mice were separated. Kyn and Trp levels were determined by LC−MS, and the Kyn/Trp ratios were calculated: control (roundness), **5a**-treated mice (regular triangle), or 1-L-MT-treated mice (square) (n = 4−6 mice/group); (∗) $P < 0.05$; (∗∗) $P < 0.01$; ns, not significant.

at room temperature. Then water (50 mL) was added and extracted with dichloromethane (3 × 10 mL). The organic layer was combined, washed with water (3 × 10 mL), dried over Na_2SO_4, and concentrated in vacuum to afford the crude product, which was purified by column chromatography on silica gel using dichloromethane/methanol (100:0 → 20:1) to give **5a**−**f**.

DOI: 10.1021/acs.jmedchem.9b01079
J. Med. Chem. XXXX, XXX, XXX−XXX

8-Fluoro-2-((4-methylpiperazin-1-yl)methyl)indolo[2,1-*b*]-quinazoline-6,12-dione (5a). Yellow solid (246 mg, 65%). ^{1}H NMR (400 MHz, $CDCl_3$) δ 8.65 (dd, J = 8.8, 4.0 Hz, 1H), 8.37 (d, J = 1.5 Hz, 1H), 7.99 (d, J = 8.3 Hz, 1H), 7.88 (dd, J = 8.3, 1.8 Hz, 1H), 7.60 (dd, J = 6.5, 2.7 Hz, 1H), 7.48−7.58 (m, 1H), 3.72 (s, 2H), 2.62 (s, 8H), 2.40 (s, 3H). ^{13}C NMR (100 MHz, $CDCl_3$) δ 181.71, 162.35, 159.87, 157.91, 145.62, 144.05, 142.30, 136.00, 130.83, 127.41, 124.79, 123.42, 119.68, 112.16, 111.92, 62.19, 55.02, 53.02, 45.93. HRMS (ESI): $[M + H]^+$ m/z 379.1566 (calcd 379.1565 for $C_{21}H_{20}FN_4O_2$).

(8-Fluoro-6-oxo-2-(piperazin-1-ylmethyl)indolo[2,1-*b*]-quinazolin-12(6*H*)-ylidene)oxonium (5b). Yellow solid (128 mg, 35%). ^{1}H NMR (400 MHz, DMSO-d_6) δ 8.47 (dd, J = 8.7, 4.0 Hz, 1H), 8.22 (d, J = 14.5 Hz, 1H), 7.88−7.93 (m, 2H), 7.78 (dd, J = 6.9, 2.3 Hz, 1H), 7.70−7.77 (m, 1H), 3.71 (s, 2H), 3.05 (s, 3H), 2.60 (s, 3H). ^{13}C NMR (100 MHz, DMSO-d_6) δ 182.00, 161.96, 159.52, 157.95, 145.99, 145.50, 142.71, 140.71, 136.26, 130.43, 127.19, 124.42, 123.48, 119.24, 112.03, 61.28, 50.35, 43.79. HRMS (ESI): $[M + H]^+$ m/z 365.1407 (calcd 365.1408 for $C_{20}H_{18}FN_4O_2$).

(2-((4-(*tert*-Butoxycarbonyl)piperazin-1-yl)methyl)-8-fluoro-6-oxoindolo[2,1-*b*]quinazolin-12(6*H*)-ylidene)oxonium (5c). Yellow solid (246 mg, 53%). ^{1}H NMR (400 MHz, $CDCl_3$) δ 8.63 (dd, J = 8.8, 4.0 Hz, 1H), 8.35 (d, J = 1.1 Hz, 1H), 7.98 (d, J = 8.3 Hz, 1H), 7.87 (dd, J = 8.3, 1.6 Hz, 1H), 7.57 (dd, J = 6.5, 2.6 Hz, 1H), 7.48 (td, J = 8.6, 2.7 Hz, 1H), 3.69 (s, 2H), 3.45−3.48 (m, 4H), 2.46 (d, 4H), 1.46 (s, 9H). ^{13}C NMR (100 MHz, $CDCl_3$) δ 181.65, 162.36, 160.91, 159.87, 157.86, 154.74, 145.69, 144.11, 142.10, 135.91, 130.88, 127.39, 124.79, 123.43, 119.67, 112.03, 79.72, 62.28, 52.96, 42.71, 28.39. HRMS (ESI): $[M + H]^+$ m/z 465.1935 (calcd 465.1933 for $C_{25}H_{26}FN_4O_4$).

2-((4-Methylpiperazin-1-yl)methyl)indolo[2,1-*b*]-quinazoline-6,12-dione (5d). Yellow solid (223 mg, 62%). ^{1}H NMR (400 MHz, $CDCl_3$) δ 8.65 (d, J = 8.1 Hz, 1H), 8.39 (s, 1H), 8.00 (d, J = 8.2 Hz, 1H), 7.93 (d, J = 7.5 Hz, 1H), 7.87 (d, J = 8.3 Hz, 1H), 7.81 (t, J = 7.8 Hz, 1H), 7.45 (t, J = 7.5 Hz, 1H), 3.71 (s, 2H), 2.60 (s, 8H), 2.37 (s, 3H). ^{13}C NMR (100 MHz, DMSO-d_6) δ 182.85, 158.11, 146.45, 146.23, 145.30, 140.53, 138.24, 136.18, 130.39, 127.41, 127.20, 125.20, 123.59, 122.72, 117.49, 60.79, 53.65, 50.61, 43.61. HRMS (ESI): $[M + H]^+$ m/z 361.1657 (calcd 361.1659 for $C_{21}H_{21}N_4O_2$).

2-((Dimethylamino)methyl)-8-fluoroindolo[2,1-*b*]-quinazoline-6,12-dione (5e). Yellow solid (217 mg, 67%). ^{1}H NMR (400 MHz, $CDCl_3$) δ 8.64 (dd, J = 8.8, 4.0 Hz, 1H), 8.34 (s, 1H), 7.98 (d, J = 8.3 Hz, 1H), 7.87 (dd, J = 8.2, 1.3 Hz, 1H), 7.58 (dd, J = 6.5, 2.5 Hz, 1H), 7.49 (td, J = 8.6, 2.6 Hz, 1H), 3.62 (s, 2H), 2.31 (s, 6H). ^{13}C NMR (100 MHz, $CDCl_3$) δ 181.68, 162.34, 159.86, 157.89, 145.64, 144.08, 142.53, 136.05, 130.86, 127.44, 124.64, 123.39, 119.69, 112.01, 63.61, 45.41, 29.63. HRMS (ESI): $[M + H]^+$ m/z 324.1146 (calcd 324.1143 for $C_{18}H_{15}N_3O_2$).

8-Fluoro-2-(morpholinomethyl)indolo[2,1-*b*]quinazoline-6,12-dione (5f). Yellow solid (171 mg, 47%). ^{1}H NMR (400 MHz, $CDCl_3$) δ 8.63 (dd, J = 8.7, 4.0 Hz, 1H), 8.36 (s, 1H), 7.98 (d, J = 8.2 Hz, 1H), 7.88 (d, J = 8.2 Hz, 1H), 7.70−7.52 (m, 1H), 7.49 (td, J = 8.6, 2.4 Hz, 1H), 3.74−3.76 (m, 3H), 3.69 (s, 2H), 2.51 (s, 4H). ^{13}C NMR (100 MHz, $CDCl_3$) δ 181.63, 162.36, 159.87, 157.87, 145.69, 144.11, 142.39, 141.63, 136.00, 130.85, 127.46, 124.79, 123.42, 119.67, 112.04, 66.92, 62.63, 53.62. HRMS (ESI): $[M + H]^+$ m/z 366.1249 (calcd 366.1248 for $C_{20}H_{17}N_3O_3$).

General Procedure for the Synthesis of *N*-Aryl Substituted Tryptanthrin Derivatives (9a−f). A suspension of 2-bromo-8-fluoroindolo[2,1-*b*]quinazoline-6,12-dione or 2-bromoindolo[2,1-*b*]-quinazoline- 6,12-dione (1 mmol), amine (2 mmol), $Pd(OAc)_2$ (67 mg, 0.3 mmol), BINAP (311 mg, 0.5 mmol), and Cs_2CO_3 (650 mg, 2 mmol) in dried toluene (15 mL) was stirred at 110 °C for 16 h under N_2. After removal of the solvent in vacuum, the residue was dissolved in dichloromethane (50 mL), washed with water (3 × 15 mL), dried over Na_2SO_4, and concentrated in vacuum to provide the crude product, which was purified by column chromatography on silica gel using dichloromethane/methanol (20:1 → 10:1) to give **9a−f**.

8-Fluoro-2-(4-methylpiperazin-1-yl)indolo[2,1-*b*]-quinazoline-6,12-dione (9a). Red solid (266 mg, 73%). ^{1}H NMR (400 MHz, $CDCl_3$) δ 8.59 (dd, J = 8.8, 4.1 Hz, 1H), 7.85 (d, J = 9.1 Hz, 1H), 7.70 (d, J = 2.9 Hz, 1H), 7.54 (dd, J = 6.6, 2.7 Hz, 1H), 7.43 (td, J = 8.7, 2.7 Hz, 1H), 7.35 (dd, J = 9.1, 2.9 Hz, 1H), 3.49 (t, 4H), 2.61 (t, 4H), 2.39 (s, 3H). ^{13}C NMR (100 MHz, $CDCl_3$) δ 181.28, 162.22, 159.74, 157.87, 152.08, 142.00, 141.38, 138.08, 132.29, 124.95, 124.11, 121.59, 119.52, 111.63, 109.84, 54.61, 47.42, 45.10. HRMS (ESI): $[M + H]^+$ m/z 365.1407 (calcd 365.1408 for $C_{20}H_{18}N_4O_2$).

8-Fluoro-2-(piperazin-1-yl)indolo[2,1-*b*]quinazoline-6,12-dione (9b). Red solid (140 mg, 40%). ^{1}H NMR (400 MHz, $CDCl_3$) δ 8.63 (dd, J = 8.8, 4.0 Hz, 1H), 7.89 (d, J = 9.0 Hz, 1H), 7.75 (d, J = 2.8 Hz, 1H), 7.57 (dd, J = 6.6, 2.5 Hz, 1H), 7.46 (td, J = 8.7, 2.6 Hz, 1H), 7.38 (dd, J = 9.1, 2.8 Hz, 1H), 3.45 (t, 4H), 3.09. ^{13}C NMR (100 MHz, $CDCl_3$) δ 181.35, 162.25, 157.96, 152.53, 142.02, 141.29, 138.11, 132.31, 125.00, 124.25, 121.62, 119.55, 111.59, 111.54, 109.81, 48.61, 45.81. HRMS (ESI): $[M + H]^+$ m/z 351.1250 (calcd 351.1252 for $C_{19}H_{16}N_4O_2$).

8-Fluoro-2-(piperidin-1-yl)indolo[2,1-*b*]quinazoline-6,12-dione (9c). Red solid (265 mg, 76%). ^{1}H NMR (400 MHz, $CDCl_3$) δ 8.64 (dd, J = 8.8, 4.1 Hz, 1H), 7.87 (d, J = 9.1 Hz, 1H), 7.74 (d, J = 3.0 Hz, 1H), 7.57 (dd, J = 6.7, 2.7 Hz, 1H), 7.46 (td, J = 8.7, 2.7 Hz, 1H), 7.36 (dd, J = 9.1, 3.0 Hz, 1H), 3.51 (d, J = 5.6 Hz, 4H), 1.74 (s, 6H). ^{13}C NMR (100 MHz, $CDCl_3$) δ 181.22, 162.19, 159.71, 157.96, 152.28, 141.92, 140.97, 137.31, 132.38, 125.07, 124.08, 121.46, 119.53, 111.53, 109.52, 48.75, 25.35, 24.25. HRMS (ESI): $[M + H]^+$ m/z 350.1301 (calcd 350.1299 for $C_{20}H_{17}N_3O_2$).

2-(4-Methylpiperazin-1-yl)indolo[2,1-*b*]quinazoline-6,12-dione (9d). Red solid (197 mg, 57%). ^{1}H NMR (400 MHz, $CDCl_3$) δ 8.58 (d, J = 8.1 Hz, 1H), 7.86 (t, J = 8.9 Hz, 2H), 7.73 (dd, J = 14.8, 5.6 Hz, 2H), 7.32−7.40 (m, 2H), 3.48 (d, J = 4.4 Hz, 4H), 2.61 (d, J = 4.8 Hz, 4H), 2.38 (s, 3H). ^{13}C NMR (100 MHz, $CDCl_3$) δ 182.26, 158.10, 151.93, 145.90, 141.48, 138.29, 137.61, 132.07, 126.86, 125.00, 124.92, 122.63, 121.70, 117.86, 109.95, 54.61, 47.48, 46.09. HRMS (ESI): $[M + H]^+$ m/z 347.1502 (calcd 347.1503 for $C_{20}H_{19}N_4O_2$).

2-(Dimethylamino)-8-fluoroindolo[2,1-*b*]quinazoline-6,12-dione (9e). Red solid (211 mg, 68%). ^{1}H NMR (400 MHz, $CDCl_3$) δ 8.63 (dd, J = 8.8, 4.1 Hz, 1H), 7.87 (d, J = 9.1 Hz, 1H), 7.53−7.57 (m, 2H), 7.45 (td, J = 8.7, 2.7 Hz, 1H), 7.17 (dd, J = 9.1, 3.0 Hz, 1H), 3.20 (s, 6H). ^{13}C NMR (100 MHz, $CDCl_3$) δ 181.24, 161.78, 160.13, 158.08, 151.50, 141.91, 140.45, 136.46, 132.50, 125.04, 124.17, 119.51, 118.99, 111.54, 107.14, 40.43. HRMS (ESI): $[M + H]^+$ m/z 310.0985 (calcd 310.0986 for $C_{17}H_{13}N_3O_2$).

8-Fluoro-2-morpholinoindolo[2,1-*b*]quinazoline-6,12-dione (9f). Red solid (214 mg, 61%). ^{1}H NMR (400 MHz, $CDCl_3$) δ 8.65 (dd, J = 8.8, 4.1 Hz, 1H), 7.93 (d, J = 9.0 Hz, 1H), 7.77 (d, J = 2.7 Hz, 1H), 7.58 (dd, J = 6.7, 2.7 Hz, 1H), 7.48 (td, J = 11.4, 5.7, 2.5 Hz, 1H), 7.39 (dd, J = 9.1, 3.0 Hz, 1H), 3.93 (t, 4H), 3.46 (t, 4H). ^{13}C NMR (100 MHz, $CDCl_3$) δ 181.38, 160.24, 157.93, 152.28, 142.10, 141.70, 138.65, 132.34, 125.02, 124.32, 124.16, 121.54, 119.61, 111.75, 109.89, 66.47, 47.68. HRMS (ESI): $[M + H]^+$ m/z 352.1093 (calcd 352.1092 for $C_{19}H_{15}FN_3O_3$).

CPMG and STD NMR Assays of Interactions between 5a and hIDO1, hIDO2, hTDO. Samples used in the NMR experiments: 200 μM compound without or with the presence of 5 μM protein. Buffer conditions: 20 mM sodium phosphate buffer, 100 mM NaCl, 5% DMSO, pH 7.4. All NMR data for the compound without or with the presence of target protein were collected on Bruker Avance III 600 MHz NMR spectrometer equipped with cryogenically cooled probe at 25 °C.

Heme Binding Studies. Optical absorption spectra of FeIII-hIDO1 (187.5 μM) were recorded with or without inhibitor treatment (375 μM) under normal atmospheric conditions in 50 mM KPB (pH 6.5) using a UV−visible spectrophotometer (Thermo Fisher Scientific, USA, path length of 1 mm).

Enzymatic IDO1, TDO, and IDO2 Inhibition Assay Based on Detection of Kynurenine.[29,39,40] In vitro enzymatic IDO1, TDO, and IDO2 inhibition assays were determined in a commonly used system with respective modification, which are described in the Table 1. Briefly, a standard reaction mixture (0.5 mL) containing all reagents

DOI: 10.1021/acs.jmedchem.9b01079
J. Med. Chem. XXXX, XXX, XXX−XXX

and hIDO1 (4−10 μg), hTDO (4−10 μg), or hIDO2 (350 μg) was added to the solution containing the test sample at a determined concentration. The reaction was carried out at 37 °C for 30 min and stopped by adding 200 μL of 30% (w/v) trichloroacetic acid (TCA). After heating at 65 °C for 15 min, the reaction mixture was centrifuged at 12 000 rpm for 10 min. The supernatant (100 μL) was transferred into a well of a 96-well microplate and mixed with 100 μL of 0.3% (w/v) *p*-dimethylaminobenzaldehyde (DMAB) in acetic acid. The yellow pigment derived from Kyn was measured at 492 nm using a SPECTRAmax250 microplate reader (Molecular Devices, USA). Enzymatic IC_{50} values were determined via nonlinear regression analysis using GraphPad Prism 5.

Cell Culture. HeLa, U87 MG, HEK293, H22, and LLC cells were authenticated by short tandem repeat analysis and passaged for fewer than 6 months before experiments. All cell lines were tested to be negative for mycoplasma contamination. The cells were cultured in DMEM (Gibco, USA) supplement with 10% (v/v) fetal bovine serum (FBS, Gibco, USA), 1% (v/v) nonessential amino acid solution (Gibco, USA), 100 μg/mL penicillin, and streptomycin (Gibco, USA) at 37 °C in an atmosphere of 5% CO_2 and 95% relative humidity.

Cellular IDO1 Inhibition Assay. In vitro cellular IDO1 inhibition assay was performed as previously described[29,41] with some modifications, which are described in the Table 2. HeLa cells were cultured in DMEM medium with 10% FBS, 1% pen/strep, 1% nonessential amino acid, 1 mM Na-pyruvate. Cells were seeded at 25 000 cells per well into 96-well microplate in 100 μL of growth medium and incubated at 37 °C and 5% CO_2 overnight. The next day 100 μL per well of diluted inhibitor in growth medium was added at a final concentration of 100 ng/mL human IFN-γ. Cells were incubated at 37 °C in a CO_2 incubator for 18 h. The next day 140 μL of medium was removed into a new 96-well plate and 10 μL of 6.1 N TCA was added. The plate was incubated at 50 °C for 30 min to hydrolyze NFK produced by IDO1 to Kyn. The plate was then centrifuged at 2500 rpm for 10 min to remove sediments. 100 μL of supernatant per well was transferred to another 96-well plate and mixed with 100 μL of 2% (w/v) DMAB in acetic acid. The plate was incubated at rt for 10 min. The yellow color derived from Kyn was recorded by measuring absorbance at 492 nm using a Multiscan spectrum Mk3 (Thermo Fisher Scientific, USA). Cellular IC_{50} values were determined via nonlinear regression analysis using GraphPad Prism 5.

Cellular TDO and IDO2 Inhibition Assays. In vitro cellular TDO and IDO2 inhibition assays were performed as previously described[39,40] that are shown in the Table 2. U87 MG and HEK293 cells were cultivated in DMEM containing 50 U/mL penicillin, 50 mg/mL streptomycin, 4500 mg/L glucose, and 10% inactivated FBS (Gibco, USA) at 37 °C with 5% CO_2 and 95% humidity. When 80% confluence was reached, cells were transfected with pcDNA3.1(+)-hIDO2 or pcDNA3.1(+)-hTDO using the transfection reagent Lipofectamine 2000 according to the manufacturer's instructions. An empty pcDNA3.1(+) expression vector served as control. After 18 h of incubation, the transfected cells were seeded in 96-well culture plates at a density of 2.5×10^4 cells/well and supplemented with 200 μM L-Trp in a final volume of 200 μL. A serial dilution of the tested compounds was added to the culture medium after an additional 6 h (IDO2) or 12 h (TDO) of incubation. The reaction was terminated by addition of 30% (w/v) TCA (10 μL for 140 μL of the reaction mixture) 24 h (IDO2) or 8 h (TDO) later. The plates were incubated at 65 °C in water bath for 15 min to facilitate the transformation of NFK to Kyn, followed by centrifugation at 13 000*g* for 10 min to remove the sediments. An amount of 100 μL of the supernatant was then transferred to another 96-well plate and mixed with a same volume of 0.3% (w/v) DMAB in acetic acid. The percentages of inhibition of Trp degradation or Kyn production by the compounds were calculated by measuring the absorption at 492 nm using a Multiscan spectrum Mk3 (Thermo Fisher Scientific, USA). Cellular IC_{50} values were determined via nonlinear regression analysis using GraphPad Prism 5.

T Cell Proliferation Assay. Blood samples of healthy volunteers were obtained from Changhai Hospital after informed consent. All procedures were approved by the Medical Ethics Committee of Fudan University. Human peripheral blood mononuclear cells (PBMCs) were isolated by centrifugation using Lymphoprep (Axis Shield, Norway) following the manufacturer's guidelines. Briefly, blood was collected into a tube containing anticoagulant (15 mg/mL ethylenediaminetetraacetic acid, EDTA), and the blood was diluted by addition of an equal volume of 0.9% NaCl. The 6 mL of diluted blood was carefully layered on the 3 mL of the prepared Lymphoprep medium, then centrifugated at 800*g* for 20 min at room temperature. After centrifugation the mononuclear cells form a distinct band at the sample/medium interface. The cells are best removed from the interface using a Pasteur pipet without removing the upper layer. The harvested fraction was diluted with 0.9% NaCl to reduce the density of the solution and pellet the cells by centrifugation at 250*g* for 10 min.

Coculture of mixed lymphocyte and HeLa cells was performed as previously described with some modifications.[41] Briefly, the lymphocyte was labeled with CFSE dye, according to CFSE cell proliferation and cell tracking kit (Yeasen, China) instructions. Stimulator ratio of 5: l (1×10^6 lymphocyte cells/well; 2×10^5 HeLa cells/well) in culture medium consisted of 150 U/mL IL-2 (Sino Biological, China), 100 ng/mL anti-CD3 (BD Biosciences, USA), and 60 ng/mL IFN-γ (Sino Biological, China) in 6-well cell culture plates (Nunc, Denmark). Meanwhile, 1-L-MT (1 μM) or **5a** of different concentration gradients (40 nM, 200 nM, 500 nM, 1 μM) was added to culture plates. After a two-day incubation, cell proliferation was measured by flow cytometer (Beckman Gallios, USA) with FL1 and FL2 channels.

Animal Model and Treatments. The 6- to 8-week-old female C57BL/6, Kunming mice and SD rats used for the study were purchased from Shanghai Laboratory Animal Center, CAS.

LLC tumor-bearing mice and H22 tumor-bearing mice were constructed as described previously with some modifications.[29,66] H22 cells (2×10^6 cells of each mouse) were inoculated into the abdomen of Kunming mice and the ascites tumor cells were passaged two times in the mice. After 1 week, the ascites tumor was collected and diluted with normal saline. LLC cells and H22 ascites tumor cells were injected sc into the right forelimb at 2×10^6 of each C57BL/6 and Kunming mouse, respectively. After the implantation, the mice were randomized into several groups: control, **5a**, and 1-L-MT. Tumor growth was monitored every 2 days. Perpendicular diameters of the tumors were measured using vernier scale calipers, and the tumor volume was calculated as follows: tumor size = long diameter × (short diameter)^2/2. When the primary tumor diameter had reached 5 mm, therapy was initiated. The mice were treated orally once daily with 0.5% CMC-Na (control), **5a** (45 mg/kg in 0.5% CMC-Na), or 1-L-MT (100 mg/kg in 0.5% CMC-Na). After 2 weeks of treatment, the mice were sacrificed, the tumors were dissected and weighed, and the blood was harvested.

LPS stimulation of KP was performed in C57BL/6 mice as previously described[67,68] with some modifications. Briefly, mice were injected ip with saline or *Escherichia coli* LPS (5 mg/kg). 24 h after modeling (ip LPS), mice were treated with 0.5% CMC-Na (0.2 mL/18 g, ig) or **5a** (60 mg/kg, ig). After 0.5% CMC-Na or **5a** treatment, the mice were sacrificed and the blood was harvested at different sampling times (1 h, 6 h, 12 h, 24 h, 30 h).

Naive SD rats were randomized into two groups of control and **5a**. The rats were treated with a single dose of 0.5% CMC-Na (control) or **5a** (30 mg/kg in 0.5% CMC-Na). The rats were sacrificed and the lung tissues were dissected.

HPLC Analysis. In vivo PD (pharmacodynamics) efficacy was evaluated by measuring the concentrations of Trp and Kyn in the serum using an Agilent 1260 series HPLC system (Agilent Corp, USA) equipped with a quad pump and a UV detector. The detection wavelengths were 280 and 360 nm. HPLC analysis of the samples was performed using an Agilent C18 column (5 μm particle size, *L* × i.d. 25 cm × 4.6 mm) preceded by a C18 guard column (Dikma, China). The mobile phase was 15 mM sodium acetate (pH 3.6) containing 4% acetonitrile.

LC−MS Analysis. In vivo PD effect of **5a** was evaluated by measuring the concentrations of Trp and Kyn in the tumors using an

DOI: 10.1021/acs.jmedchem.9b01079
J. Med. Chem. XXXX, XXX, XXX−XXX

Agilent 1100 LC−MS spectrometer. Agilent ZORBAX SB-C18 (2.1 mm × 150 mm, 5 μm) was used for separation. The precolumn was a Waters Xterra MS C18 Guard column (2.1 mm × 10 mm). The mobile phase was acetonitrile and 0.1% formic acid. The acetonitrile ratio was 5−80% gradient elution. The analysis time was 5 min, postcolumn equilibrium was performed for 3 min, the flow rate was 0.7 mL/min, the column temperature was 35 °C. The mass-to-charge ratios of the Kyn, Trp, and internal standard metronidazole were respectively 209, 205, and 172. The signal modes were positive ion modes.

Ethics Approval and Consent To Participate. The 6- to 8-week-old female C57BL/6, Kunming mice and SD rats used for the study were purchased from Shanghai Laboratory Animal Center, CAS. The use of animal was approved by the Animal Ethics Committee of Fudan University, and experiments were performed in compliance with ARRIVE guidelines. Blood samples of healthy volunteers were obtained from Changhai Hospital after informed consent. All procedures were approved by the Changhai Hospital Ethics Committee.

Statistical Analysis. Data are expressed as mean values ± SD or SEM. The one-way ANOVA method and two-way ANOVA method were used to determine the statistical significance of the differences observed between the control and the test-compound-treated groups of mice. GraphPad Prism 5 was used to create the graphs and implement the statistical analysis. Enzymatic and cellular IC_{50} values were determined via nonlinear regression analysis using GraphPad Prism 5. Significance values were set at (*) $P < 0.05$, (**) $P < 0.01$, (***) $P < 0.001$.

■ ASSOCIATED CONTENT

Supporting Information

The Supporting Information is available free of charge on the ACS Publications website at DOI: 10.1021/acs.jmedchem.9b01079.

Molecular formula strings and some data (CSV)

General materials, general protocols of in vitro biological assay, ^{1}H and ^{13}CNMR spectra of tested compounds, and HPLC spectra data for the purity of compound **5a** (PDF)

■ AUTHOR INFORMATION

Corresponding Authors

*C.K.: e-mail, kuangcx@tongji.edu.cn; telephone and fax, +86-021-65982351.

*Q.Y.: e-mail, yangqing68@fudan.edu.cn; telephone and fax, +86-021-31246641.

ORCID

Qing Yang: 0000-0003-4162-922X

Author Contributions

D.Y. performed most of the enzymatic, cellular, CPMG and STD NMR and animal experiments. S.Z. partially contributed to enzymatic, cellular, and animal experiments. X.F. partially contributed to enzymatic, cellular, and CPMG and STD NMR experiments. L.G., N.H., and Z.G. partially contributed to animal experiments. S.Y., X.L., and J.C.H partially contributed to enzymatic and cellular experiments. C.K. synthesized tryptanthrins and analyzed chemistry and structure-related results. Q.Y. and C.K. initiated the research, led the project team, designed experiments, analyzed results, and wrote the manuscript. All authors have given approval to the final version of the manuscript.

Notes

The authors declare no competing financial interest.

■ ACKNOWLEDGMENTS

We thank Changhui Su for providing constructive suggestions on the writing. This work was supported by National Key R&D Program of China (Grant 2016YFC1303503) and the Key Biomedical Program of Shanghai (Grants 17431902200 and 18431902600).

■ ABBREVIATIONS USED

IDO1, indoleamine 2,3-dioxygenase 1; IDO2, indoleamine 2,3-dioxygenase 2; TDO, tryptophan 2,3-dioxygenase; Trp, tryptophan; Kyn, kynurenine; 5-HT, serotonin; KP, kynurenine pathway; CNS, central nervous system; QUIN, quinolinic acid; AhR, aryl hydrocarbon receptor; K_i, inhibition constant; IFN-γ, interferon-γ; NFK, *N*-formyl kynurenine; KPB, potassium phosphate buffer; CPMG, Carr−Purcell−Meiboom−Gill; STD, saturation transfer difference; FBS, fetal bovine serum; EDTA, ethylenediaminetetraacetic acid; ESI, electrospray ionization mass spectra; DMAB, *p*-dimethylaminobenzaldehyde; TCA, trichloroacetic acid

■ REFERENCES

(1) Ruddick, J. P.; Evans, A. K.; Nutt, D. J.; Lightman, S. L.; Rook, G. A.; Lowry, C. A. Tryptophan metabolism in the central nervous system: medical implications. *Expert Rev. Mol. Med.* **2006**, *8* (20), 1−27.

(2) Schwarcz, R.; Bruno, J. P.; Muchowski, P. J.; Wu, H. Q. Kynurenines in the mammalian brain: when physiology meets pathology. *Nat. Rev. Neurosci.* **2012**, *13* (7), 465−477.

(3) Kolodziej, L. R.; Paleolog, E. M.; Williams, R. O. Kynurenine metabolism in health and disease. *Amino Acids* **2011**, *41* (5), 1173−1183.

(4) Ball, H. J.; Jusof, F. F.; Bakmiwewa, S. M.; Hunt, N. H.; Yuasa, H. J. Tryptophan-catabolizing enzymes - party of three. *Front. Immunol.* **2014**, *5* (485), 1−10.

(5) Moffett, J. R.; Namboodiri, M. A. Tryptophan and the immune response. *Immunol. Cell Biol.* **2003**, *81* (4), 247−265.

(6) Yu, C. P.; Song, Y. L.; Zhu, Z. M.; Huang, B.; Xiao, Y. Q.; Luo, D. Y. Targeting TDO in cancer immunotherapy. *Med. Oncol.* **2017**, *34* (5), 73−81.

(7) Zhai, L.; Spranger, S.; Binder, D. C.; Gritsina, G.; Lauing, K. L.; Giles, F. J.; Wainwright, D. A. Molecular pathways: targeting IDO1 and other tryptophan dioxygenases for cancer immunotherapy. *Clin. Cancer Res.* **2015**, *21* (24), 5427−5433.

(8) Kanai, M.; Funakoshi, H.; Takahashi, H.; Hayakawa, T.; Mizuno, S.; Matsumoto, K.; Nakamura, T. Tryptophan 2,3-dioxygenase is a key modulator of physiological neurogenesis and anxiety-related behavior in mice. *Mol. Brain* **2009**, *2* (8), 8−23.

(9) Ball, H. J.; Sanchez-Perez, A.; Weiser, S.; Austin, C. J.; Astelbauer, F.; Miu, J.; McQuillan, J. A.; Stocker, R.; Jermiin, L. S.; Hunt, N. H. Characterization of an indoleamine 2,3-dioxygenase-like protein found in humans and mice. *Gene* **2007**, *396* (1), 203−213.

(10) Metz, R.; Duhadaway, J. B.; Kamasani, U.; Laury-Kleintop, L.; Muller, A. J.; Prendergast, G. C. Novel tryptophan catabolic enzyme IDO2 is the preferred biochemical target of the antitumor indoleamine 2,3-dioxygenase inhibitory compound D-1-methyl-tryptophan. *Cancer Res.* **2007**, *67* (15), 7082−7087.

(11) Yuasa, H. J.; Takubo, M.; Takahashi, A.; Hasegawa, T.; Noma, H.; Suzuki, T. Evolution of vertebrate indoleamine 2,3-dioxygenases. *J. Mol. Evol.* **2007**, *65* (6), 705−714.

(12) Metz, R.; Smith, C.; DuHadaway, J. B.; Chandler, P.; Baban, B.; Merlo, L. M.; Pigott, E.; Keough, M. P.; Rust, S.; Mellor, A. L.; Mandik-Nayak, L.; Muller, A. J.; Prendergast, G. C. IDO2 is critical for IDO1-mediated T-cell regulation and exerts a non-redundant function in inflammation. *Int. Immunol.* **2014**, *26* (7), 357−367.

(13) Merlo, L. M. F.; Pigott, E.; DuHadaway, J. B.; Grabler, S.; Metz, R.; Prendergast, G. C.; Mandik-Nayak, L. IDO2 is a critical mediator

DOI: 10.1021/acs.jmedchem.9b01079
J. Med. Chem. XXXX, XXX, XXX−XXX

of autoantibody production and inflammatory pathogenesis in a mouse model of autoimmune arthritis. *J. Immunol.* **2014**, *192* (5), 2082−2090.
(14) Too, L. K.; Li, K. M.; Suarna, C.; Maghzal, G. J.; Stocker, R.; McGregor, I. S.; Hunt, N. H. Deletion of TDO2, IDO-1 and IDO-2 differentially affects mouse behavior and cognitive function. *Behav. Brain Res.* **2016**, *312*, 102−117.
(15) Qian, S.; Zhang, M.; Chen, Q. L.; He, Y. Y.; Wang, W.; Wang, Z. Y. IDO as a drug target for cancer immunotherapy: recent developments in IDO inhibitors discovery. *RSC Adv.* **2016**, *6* (9), 7575−7581.
(16) Opitz, C. A.; Litzenburger, U. M.; Sahm, F.; Ott, M.; Tritschler, I.; Trump, S.; Schumacher, T.; Jestaedt, L.; Schrenk, D.; Weller, M.; Jugold, M.; Guillemin, G. J.; Miller, C. L.; Lutz, C.; Radlwimmer, B.; Lehmann, I.; von Deimling, A.; Wick, W.; Platten, M. An endogenous tumour-promoting ligand of the human aryl hydrocarbon receptor. *Nature* **2011**, *478* (7368), 197−203.
(17) Prendergast, G. C.; Metz, R.; Muller, A. J.; Merlo, L. M.; Mandik-Nayak, L. IDO2 in immunomodulation and autoimmune disease. *Front. Immunol.* **2014**, *5* (585), 1−6.
(18) Platten, M.; Litzenburger, U.; Wick, W. The aryl hydrocarbon receptor in tumor immunity. *Oncoimmunology* **2012**, *1* (3), 396−397.
(19) Lob, S.; Konigsrainer, A.; Rammensee, H. G.; Opelz, G.; Terness, P. Inhibitors of indoleamine-2,3-dioxygenase for cancer therapy: can we see the wood for the trees? *Nat. Rev. Cancer* **2009**, *9* (6), 445−452.
(20) Muller, A. J.; DuHadaway, J. B.; Donover, P. S.; Sutanto-Ward, E.; Prendergast, G. C. Inhibition of indoleamine 2,3-dioxygenase, an immunoregulatory target of the cancer suppression gene Bin1, potentiates cancer chemotherapy. *Nat. Med.* **2005**, *11* (3), 312−319.
(21) Koblish, H. K.; Hansbury, M. J.; Bowman, K. J.; Yang, G.; Neilan, C. L.; Haley, P. J.; Burn, T. C.; Waeltz, P.; Sparks, R. B.; Yue, E. W.; Combs, A. P.; Scherle, P. A.; Vaddi, K.; Fridman, J. S. Hydroxyamidine inhibitors of indoleamine-2,3-dioxygenase potently suppress systemic tryptophan catabolism and the growth of IDO-expressing tumors. *Mol. Cancer Ther.* **2010**, *9* (2), 489−498.
(22) Banerjee, T.; DuHadaway, J. B.; Gaspari, P.; Sutanto-Ward, E.; Munn, D. H.; Mellor, A. L.; Malachowski, W. P.; Prendergast, G. C.; Muller, A. J. A key in vivo antitumor mechanism of action of natural product-based brassinins is inhibition of indoleamine 2,3-dioxygenase. *Oncogene* **2008**, *27* (20), 2851−2857.
(23) Gaspari, P.; Banerjee, T.; Malachowski, W. P.; Muller, A. J.; Prendergast, G. C.; DuHadaway, J.; Bennett, S.; Donovan, A. M. Structure-activity study of Brassinin derivatives as indoleamine 2,3-dioxygenase inhibitors. *J. Med. Chem.* **2006**, *49* (2), 684−692.
(24) Carr, G.; Chung, M. K.; Mauk, A. G.; Andersen, R. J. Synthesis of indoleamine 2,3-dioxygenase inhibitory analogues of the sponge alkaloid exiguamine A. *J. Med. Chem.* **2008**, *51* (9), 2634−2637.
(25) Brastianos, H. C.; Vottero, E.; Patrick, B. O.; Van Soest, R.; Matainaho, T.; Mauk, A. G.; Andersen, R. J. Exiguamine A, an indoleamine-2,3-dioxygenase (IDO) inhibitor isolated from the marine sponge Neopetrosia exigua. *J. Am. Chem. Soc.* **2006**, *128* (50), 16046−16047.
(26) Kumar, S.; Jaller, D.; Patel, B.; LaLonde, J. M.; DuHadaway, J. B.; Malachowski, W. P.; Prendergast, G. C.; Muller, A. J. Structure based development of phenylimidazole-derived inhibitors of indoleamine 2,3-dioxygenase. *J. Med. Chem.* **2008**, *51* (16), 4968−4977.
(27) Pereira, A.; Vottero, E.; Roberge, M.; Mauk, A. G.; Andersen, R. J. Indoleamine 2,3-dioxygenase inhibitors from the northeastern pacific marine hydroid garveia annulata. *J. Nat. Prod.* **2006**, *69* (10), 1496−1499.
(28) Huang, Q.; Zheng, M. F.; Yang, S. S.; Kuang, C. X.; Yu, C. J.; Yang, Q. Structure-activity relationship and enzyme kinetic studies on 4-aryl-1H-1,2,3-triazoles as indoleamine 2,3-dioxygenase (IDO) inhibitors. *Eur. J. Med. Chem.* **2011**, *46* (11), 5680−5687.
(29) Yang, S.; Li, X.; Hu, F.; Li, Y.; Yang, Y.; Yan, J.; Kuang, C.; Yang, Q. Discovery of tryptanthrin derivatives as potent inhibitors of indoleamine 2,3-dioxygenase with therapeutic activity in lewis lung cancer (LLC) tumor-bearing mice. *J. Med. Chem.* **2013**, *56* (21), 8321−8331.
(30) Vacchelli, E.; Aranda, F.; Eggermont, A.; Sautès-Fridman, C.; Tartour, E.; Kennedy, E. P.; Platten, M.; Zitvogel, L.; Kroemer, G.; Galluzzi, L. Trial watch: IDO inhibitors in cancer therapy. *Oncoimmunology* **2014**, *3* (10), e957994.
(31) Rohrig, U. F.; Majjigapu, S. R.; Vogel, P.; Zoete, V.; Michielin, O. Challenges in the discovery of indoleamine 2,3-dioxygenase 1 (IDO1) inhibitors. *J. Med. Chem.* **2015**, *58* (24), 9421−9437.
(32) Buque, A.; Bloy, N.; Aranda, F.; Cremer, I.; Eggermont, A.; Fridman, W. H.; Fucikova, J.; Galon, J.; Spisek, R.; Tartour, E.; Zitvogel, L.; Kroemer, G.; Galluzzi, L. Trial watch-small molecules targeting the immunological tumor microenvironment for cancer therapy. *Oncoimmunology* **2016**, *5* (6), e1149674.
(33) Pilotte, L.; Larrieu, P.; Stroobant, V.; Colau, D.; Dolusic, E.; Frédérick, R.; De Plaen, E.; Uyttenhove, C.; Wouters, J.; Masereel, B.; Van den Eynde, B. J. Reversal of tumoral immune resistance by inhibition of tryptophan 2,3-dioxygenase. *Proc. Natl. Acad. Sci. U. S. A.* **2012**, *109* (7), 2497−2502.
(34) Qian, F.; Liao, J. Q.; Villella, J.; Edwards, R.; Kalinski, P.; Lele, S.; Shrikant, P.; Odunsi, K. Effects of 1-methyltryptophan stereoisomers on IDO2 enzyme activity and IDO2-mediated arrest of human T cell proliferation. *Cancer Immunol. Immunother.* **2012**, *61* (11), 2013−2020.
(35) Dounay, A. B.; Tuttle, J. B.; Verhoest, P. R. Challenges and opportunities in the discovery of new therapeutics targeting the kynurenine pathway. *J. Med. Chem.* **2015**, *58* (22), 8762−8782.
(36) Lob, S.; Konigsrainer, A.; Schafer, R.; Rammensee, H. G.; Opelz, G.; Terness, P. Levo- but not dextro-1-methyl tryptophan abrogates the IDO activity of human dendritic cells. *Blood* **2008**, *111* (4), 2152−2154.
(37) Yuasa, H. J.; Ball, H. J.; Austin, C. J.; Hunt, N. H. 1-L-methyltryptophan is a more effective inhibitor of vertebrate IDO2 enzymes than 1-D-methyltryptophan. *Comp. Biochem. Physiol., Part B: Biochem. Mol. Biol.* **2010**, *157* (1), 10−15.
(38) Bakmiwewa, S. M.; Fatokun, A. A.; Tran, A.; Payne, R. J.; Hunt, N. H.; Ball, H. J. Identification of selective inhibitors of indoleamine 2,3-dioxygenase 2. *Bioorg. Med. Chem. Lett.* **2012**, *22* (24), 7641−7646.
(39) Li, J. J.; Li, Y.; Yang, D.; Hu, N.; Guo, Z. L.; Kuang, C. X.; Yang, Q. Establishment of a human indoleamine 2,3-dioxygenase 2 (hIDO2) bioassay system and discovery of tryptanthrin derivatives as potent hIDO2 inhibitors. *Eur. J. Med. Chem.* **2016**, *123*, 171−179.
(40) Zhang, S. N.; Qi, F. F.; Fang, X.; Yang, D.; Hu, H.; Huang, Q.; Kuang, C. X.; Yang, Q. Tryptophan 2,3-dioxygenase inhibitory activities of tryptanthrin derivatives. *Eur. J. Med. Chem.* **2018**, *160*, 133−145.
(41) Liu, X. D.; Shin, N.; Koblish, H. K.; Yang, G.; Wang, Q.; Wang, K.; Leffet, L.; Hansbury, M. J.; Thomas, B.; Rupar, M.; Waeltz, P.; Bowman, K. J.; Polam, P.; Sparks, R. B.; Yue, E. W.; Li, Y.; Wynn, R.; Fridman, J. S.; Burn, T. C.; Combs, A. P.; Newton, R. C.; Scherle, P. A. Selective inhibition of IDO1 effectively regulates mediators of antitumor immunity. *Blood* **2010**, *115* (17), 3520−3530.
(42) Seegers, N.; van Doornmalen, A. M.; Uitdehaag, J. C.; de Man, J.; Buijsman, R. C.; Zaman, G. J. High-throughput fluorescence-based screening assays for tryptophan-catabolizing enzymes. *J. Biomol. Screening* **2014**, *19* (9), 1266−1274.
(43) Abdel-Magid, A. F. Targeting the inhibition of tryptophan 2,3-dioxygenase (TDO-2) for cancer treatment. *ACS Med. Chem. Lett.* **2017**, *8* (1), 11−13.
(44) Crosignani, S.; Driessens, G.; Detheux, M.; Van den Eynde, B.; Cauwenberghs, S. Preclinical assessment of a novel small molecule inhibitor of tryptophan 2,3-dioxygenase 2 (TDO2). *J. Immunother. Cancer* **2014**, *2* (3), 196−196.
(45) Rohrig, U. F.; Majjigapu, S. R.; Caldelari, D.; Dilek, N.; Reichenbach, P.; Ascencao, K.; Irving, M.; Coukos, G.; Vogel, P.; Zoete, V.; Michielin, O. 1,2,3-Triazoles as inhibitors of indoleamine 2,3-dioxygenase 2 (IDO2). *Bioorg. Med. Chem. Lett.* **2016**, *26* (17), 4330−4333.

DOI: 10.1021/acs.jmedchem.9b01079
J. Med. Chem. XXXX, XXX, XXX−XXX

(46) Sono, M.; Cady, S. G. Enzyme kinetic and spectroscopic studies of inhibitor and effector interactions with indoleamine 2,3-dioxygenase. 1. norharman and 4-phenylimidazole binding to the enzyme as inhibitors and heme ligands. *Biochemistry* **1989**, *28* (13), 5392−5399.
(47) Sugimoto, H.; Oda, S.; Otsuki, T.; Hino, T.; Yoshida, T.; Shiro, Y. Crystal structure of human indoleamine 2,3-dioxygenase: catalytic mechanism of O2 incorporation by a heme-containing dioxygenase. *Proc. Natl. Acad. Sci. U. S. A.* **2006**, *103* (8), 2611−2616.
(48) Crosignani, S.; Bingham, P.; Bottemanne, P.; Cannelle, H.; Cauwenberghs, S.; Cordonnier, M.; Dalvie, D.; Deroose, F.; Feng, J. L.; Gomes, B.; Greasley, S.; Kaiser, S. E.; Kraus, M.; Négrerie, M.; Maegley, K.; Miller, N.; Murray, B. W.; Schneider, M.; Soloweij, J.; Stewart, A. E.; Tumang, J.; Torti, V. R.; Van Den Eynde, B.; Wythes, M. Discovery of a novel and selective indoleamine 2,3-Dioxygenase (IDO-1) inhibitor 3-(5-Fluoro-1H-indol-3-yl)pyrrolidine-2,5-dione (EOS200271/PF-06840003) and its characterization as a potential clinical candidate. *J. Med. Chem.* **2017**, *60* (23), 9617−9629.
(49) Meininger, D.; Zalameda, L.; Liu, Y.; Stepan, L. P.; Borges, L.; McCarter, J. D.; Sutherland, C. L. Purification and kinetic characterization of human indoleamine 2,3-dioxygenases 1 and 2 (IDO1 and IDO2) and discovery of selective IDO1 inhibitors. *Biochim. Biophys. Acta, Proteins Proteomics* **2011**, *1814* (12), 1947−1954.
(50) Prendergast, G. C.; Malachowski, W. P.; DuHadaway, J. B.; Muller, A. J. Discovery of IDO1 inhibitors: from bench to bedside. *Cancer Res.* **2017**, *77* (24), 6795−6811.
(51) Cady, S. G.; Sono, M. 1-Methyl-dl-Tryptophan, beta-(3-Benzofuranyl)-dl-alanine (the Oxygen analog of tryptophan), and beta-[3-benzo(b)Thienyl]-dl-alanine (the sulfur analog of tryptophan) are competitive inhibitors for indoleamine 2,3-Dioxygenase. *Arch. Biochem. Biophys.* **1991**, *291* (2), 326−333.
(52) Rohrig, U. F.; Majjigapu, S. R.; Grosdidier, A.; Bron, S.; Stroobant, V.; Pilotte, L.; Colau, D.; Vogel, P.; Van den Eynde, B.; Zoete, V.; Michielin, O. Rational design of 4-aryl-1,2,3-triazoles for indoleamine 2,3-dioxygenase 1 inhibition. *J. Med. Chem.* **2012**, *55* (11), 5270−5290.
(53) Moineaux, L.; Laurent, S.; Reniers, J.; Dolušić, E.; Galleni, M.; Frère, J. M.; Masereel, B.; Frédérick, R.; Wouters, J. Synthesis, crystal structures and electronic properties of isomers of chloro-pyridinyl-vinyl-1H-indoles. *Eur. J. Med. Chem.* **2012**, *54*, 95−102.
(54) Siu, L. L.; Gelmon, K.; Chu, Q.; Pachynski, P.; Alese, O.; Basciano, P.; Walker, J.; Mitra, P.; Zhu, L.; Phillips, P.; Hunt, J.; Desai, J. BMS-986205, an optimized indoleamine 2,3-dioxygenase 1 (IDO1) inhibitor, is well tolerated with potent pharmacodynamic (PD) activity, alone and in combination with nivolumab (nivo) in advanced cancers in a phase 1/2a trial. *Cancer Res.* **2017**, *77*, 116−121.
(55) Chauhan, N.; Thackray, S. J.; Rafice, S. A.; Eaton, G.; Lee, M.; Efimov, I.; Basran, J.; Jenkins, P. R.; Mowat, C. G.; Chapman, S. K.; Raven, E. L. Reassessment of the reaction mechanism in the heme dioxygenases. *J. Am. Chem. Soc.* **2009**, *131* (12), 4186−4187.
(56) Yue, E. W.; Sparks, R.; Polam, P.; Modi, D.; Douty, B.; Wayland, B.; Glass, B.; Takvorian, A.; Glenn, J.; Zhu, W.; Bower, M.; Liu, X.; Leffet, L.; Wang, Q.; Bowman, K. J.; Hansbury, M. J.; Wei, M.; Li, Y.; Wynn, R.; Burn, T. C.; Koblish, H. K.; Fridman, J. S.; Emm, T.; Scherle, P. A.; Metcalf, B.; Combs, A. P. INCB24360 (Epacadostat), a highly potent and selective indoleamine-2,3-dioxygenase 1 (IDO1) inhibitor for immuno-oncology. *ACS Med. Chem. Lett.* **2017**, *8* (5), 486−491.
(57) Yu, C. J.; Zheng, M. F.; Kuang, C. X.; Huang, W. D.; Yang, Q. Oren-gedoku-to and its constituents with therapeutic potential in Alzheimer's disease inhibit indoleamine 2,3-dioxygenase activity in vitro. *J. Alzheimer's Dis.* **2010**, *22* (1), 257−266.
(58) Tojo, S.; Kohno, T.; Tanaka, T.; Kamioka, S.; Ota, Y.; Ishii, T.; Kamimoto, K.; Asano, S.; Isobe, Y. Crystal structures and structure activity relationships of imidazothiazole derivatives as IDO1 inhibitors. *ACS Med. Chem. Lett.* **2014**, *5* (10), 1119−1123.
(59) Peng, Y. H.; Ueng, S. H.; Tseng, C. T.; Hung, M. S.; Song, J. S.; Wu, J. S.; Liao, F. Y.; Fan, Y. S.; Wu, M. H.; Hsiao, W. C.; Hsueh, C. C.; Lin, S. Y.; Cheng, C. Y.; Tu, C. H.; Lee, L. C.; Cheng, M. F.; Shia, K. S.; Shih, C.; Wu, S. Y. Important hydrogen bond networks in indoleamine 2,3-dioxygenase 1 (IDO1) inhibitor design revealed by crystal structures of imidazoleisoindole derivatives with IDO1. *J. Med. Chem.* **2016**, *59* (1), 282−293.
(60) Nelp, M. T.; Kates, P. A.; Hunt, J. T.; Newitt, J. A.; Balog, A.; Maley, D.; Zhu, X.; Abell, L.; Allentoff, A.; Borzilleri, R.; Lewis, H. A.; Lin, Z.; Seitz, S. P.; Yan, C.; Groves, J. T. Immune-modulating enzyme indoleamine 2,3-dioxygenase is effectively inhibited by targeting its apo-form. *Proc. Natl. Acad. Sci. U. S. A.* **2018**, *115* (13), 3249−3254.
(61) Friberg, M.; Jennings, R.; Alsarraj, M.; Dessureault, S.; Cantor, A.; Extermann, M.; Mellor, A. L.; Munn, D. H.; Antonia, S. J. Indoleamine 2,3-dioxygenase contributes to tumor cell evasion of T cell-mediated rejection. *Int. J. Cancer* **2002**, *101* (2), 151−155.
(62) Metz, R.; Rust, S.; Duhadaway, J. B.; Mautino, M. R.; Munn, D. H.; Vahanian, N. N.; Link, C. J.; Prendergast, G. C. IDO inhibits a tryptophan sufficiency signal that stimulates mTOR: A novel IDO effector pathway targeted by D-1-methyl-tryptophan. *Oncoimmunology* **2012**, *1* (9), 1460−1468.
(63) Schafer, C. C.; Wang, Y.; Hough, K. P.; Sawant, A.; Grant, S. C.; Thannickal, V. J.; Zmijewski, J.; Ponnazhagan, S.; Deshane, J. S. Indoleamine 2,3-dioxygenase regulates anti-tumor immunity in lung cancer by metabolic reprogramming of immune cells in the tumor microenvironment. *Oncotarget* **2016**, *7* (46), 75407−75424.
(64) Lemos, H.; Mohamed, E.; Huang, L.; Ou, R.; Pacholczyk, G.; Arbab, A. S.; Munn, D.; Mellor, A. L. STING promotes the growth of tumors characterized by low antigenicity via IDO activation. *Cancer Res.* **2016**, *76* (8), 2076−2081.
(65) Zhang, Y.; Fu, J.; Shi, Y.; Peng, S.; Cai, Y.; Zhan, X.; Song, N.; Liu, Y.; Wang, Z.; Yu, Y.; Wang, Y.; Shi, Q.; Fu, Y.; Yuan, K.; Zhou, N.; Joshi, R.; Ichim, T. E.; Min, W. A new cancer immunotherapy via simultaneous DC-mobilization and DC-targeted IDO gene silencing using an immune-stimulatory nanosystem. *Int. J. Cancer* **2018**, *143* (8), 2039−2052.
(66) Nie, J.; Yang, H. M.; Sun, C. Y.; Liu, Y. L.; Zhuo, J. Y.; Zhang, Z. B.; Lai, X. P.; Su, Z. R.; Li, Y. C. Scutellarin enhances antitumor effects and attenuates the toxicity of bleomycin in H22 ascites tumor-bearing mice. *Front. Pharmacol.* **2018**, *9* (615), 1−16.
(67) Miura, H.; Shirokawa, T.; Isobe, K.; Ozaki, N. Shifting the balance of brain tryptophan metabolism elicited by isolation housing and systemic administration of lipopolysaccharide in mice. *Stress* **2009**, *12* (3), 206−214.
(68) Salazar, A.; Gonzalez-Rivera, B. L.; Redus, L.; Parrott, J. M.; O'Connor, J. C. Indoleamine 2,3-dioxygenase mediates anhedonia and anxiety-like behaviors caused by peripheral lipopolysaccharide immune challenge. *Horm. Behav.* **2012**, *62* (3), 202−209.

DOI: 10.1021/acs.jmedchem.9b01079
J. Med. Chem. XXXX, XXX, XXX−XXX